
MaD-Mix: MULTI-MODAL DATA MIXTURES VIA LATENT SPACE COUPLING FOR VISION-LANGUAGE MODEL TRAINING

Wanyun Xie
 LIONS, EPFL
 wanyun.xie@epfl.ch

Francesco Tonin
 LIONS, EPFL
 francesco.tonin@epfl.ch

Volkan Cevher
 LIONS, EPFL
 volkan.cevher@epfl.ch

Abstract

Vision-Language Models (VLMs) are typically trained on a diverse set of multi-modal domains, yet current practices rely on costly manual tuning. We propose **MaD-Mix**, a principled and computationally efficient framework that derives multi-modal data mixtures for VLM training. **MaD-Mix** formulates data mixing as modality-aware domain alignment maximization and obtains closed-form multi-modal alignment scores from the Fenchel dual through inter-modal coupling variables. **MaD-Mix** systematically handles domains with missing modalities, allowing for the integration of language-only domains. Empirical evaluations across 0.5B and 7B models demonstrate that **MaD-Mix** *accelerates* VLM training across diverse benchmarks. **MaD-Mix** matches human-tuned data mixtures using 22% fewer training steps in image-text instruction tuning. In complex tri-modal video-image-text scenarios, where manual tuning becomes impractical, **MaD-Mix** boosts average accuracy over uniform weights, with negligible mixture computation overhead (<1 GPU-hour), enabling scalable mixture design for modern VLM pipelines.

1 Introduction

Vision-Language Models (VLMs) have advanced significantly with the availability of large-scale multi-modal datasets. The training data for VLMs is typically a complex mixture from numerous domains and multiple modalities (Bai et al., 2023a; Liu et al., 2023a; Li et al., 2024a; Liu et al., 2024a). For example, LLaVA-OneVision is trained on 20.6% Doc/Chart/Screen, 20.1% Math/Reasoning, and 8.9% OCR data, etc., and includes text and vision modalities (Li et al., 2024a). Since such domains help maintain and balance the skill distribution that a trained large multi-modal model should cover (Li et al., 2024a), many studies follow the topic or capability-oriented rule with domain structure when collecting data, such as LLaVA (Liu et al., 2023a; Li et al., 2024a), Qwen (Bai et al., 2023b; Yang et al., 2025), LLAMA (Dubey et al., 2024), Gemini (Team et al., 2023), InstructBLIP (Dai et al., 2023), and others (Li et al., 2025; Tong et al., 2024; Chen et al., 2024a; Laurençon et al., 2024). Moreover, the composition of these domains critically impacts VLM effectiveness (Bai et al., 2023a; Li et al., 2024a; Liu et al., 2024b; Gadre et al., 2023). “*How to systematically determine the proportions of each domain for VLM training without costly tuning?*” is an essential question and remains an open challenge.

Existing strategies for constructing multi-modal data mixtures often lack a formal methodology. Data recipes for many state-of-the-art models are not publicly released, while open-source models typically rely on expensive manual tuning or heuristic adjustments based on developers’ experience (Bai et al., 2023a; Li et al., 2024a). For instance, Flamingo relies on empirically-tuned mixtures (Alayrac et al., 2022), LLaVA-NeXT manually adds data domains to improve specific skills (Liu et al., 2024b), and InstructBLIP uses a simple sampling heuristic to handle data imbalance (Dai et al., 2023). Such approaches are inefficient and unscalable, especially as datasets grow. Consequently, a principled and efficient methodology for optimizing the data mixture for VLMs is notably absent.

Although data mixing strategies have shown considerable success in Large Language Model (LLM) training (Xie et al., 2023; Fan et al., 2024a; Liu et al., 2024c; Kang et al., 2024), directly transferring these unimodal

Correspondence to: Wanyun Xie <wanyun.xie@epfl.ch>, Francesco Tonin <francesco.tonin@epfl.ch>.

approaches to VLMs presents significant challenges due to their fundamental differences. The VLM data mixing problem introduces two unique challenges: *(i)* integrating features from **different modalities** (e.g., text and vision); and *(ii)* handling domains with **missing modalities**, which frequently arises in VLM training where some domains include text-image paired data for visual learning, while others have text-only data for preserving linguistic abilities. Therefore, a specialized, modality-aware methodology is required for effective VLM data mixing.

In this paper, we introduce **MaD-Mix**, a framework for systematically determining domain weights in VLM training. **MaD-Mix** computes modality-aware scores by casting multi-modal data mixing as a latent-space coupling objective and deriving the scores via the corresponding dual solution. We achieve cross-modal integration via shared latent variables that map multi-modal features into a common space. In addition, **MaD-Mix** handles missing modalities by explicitly decoupling them from the optimization process, ensuring they do not propagate noise into the alignment objective. The resulting scores directly translate into resampling weights, yielding higher VLM training efficiency and mitigating the cost of manual mixture tuning.

Specifically, the novelty and contribution of this work can be summarized as:

- We propose **MaD-Mix**, a principled fusion-based framework for reweighting multi-modal domains in VLM training. At the core of **MaD-Mix** is a robust fusion mechanism that derives domain weights by measuring the projection of each domain onto a shared latent space. Specifically, we show that coupling modalities via dual variables with an alignment objective leads to a weighting scheme acting as spectral soft-thresholding. We show that this formulation yields a computationally efficient closed-form solution.
- We address the challenge of heterogeneous multi-modal data integration. Our method is explicitly designed to handle domains with differing modalities (e.g., mixing image-text paired and text-only domains) by decoupling missing modalities from the objective and ensuring no noise is introduced by incomplete data.
- We empirically validate **MaD-Mix** on 0.5B and 7B VLMs, demonstrating its effectiveness and negligible cost. On the 0.5B model, it matches expert-tuned performance with a $1.28\times$ speedup in image-text tuning. In complex video-image-text scenarios, it outperforms uniform weighting using only 33% of the training steps. Notably, the computational cost of computing domain weights is less than 1 GPU-hour.

2 Related Works

Data composition in VLMs. The performance of modern VLMs is critically dependent on the composition of their training data. A standard practice in the field is to curate data into distinct, skill-oriented domains to ensure a balanced set of capabilities. For example, the development of the LLaVA family (Liu et al., 2023a; Li et al., 2024a; Liu et al., 2024a) involved explicitly adding new data domains like DocVQA and ChartQA to improve targeted skills such as OCR and chart understanding. They openly release the LLaVA-OneVision (Li et al., 2024a) datasets as collections of domain-specific data, which we use in our experiments. Similarly, the Qwen-VL (Bai et al., 2023a) and Gemini (Team et al., 2023) employ a multi-stage training pipeline that combines multi-modal data with text-only dialogue to maintain language capabilities. InstructBLIP (Gu et al., 2024a) also groups 26 public datasets into 11 categories to cover a wide variety of tasks and capabilities. Many other works (Li et al., 2025; Tong et al., 2024; Chen et al., 2024a; Laurençon et al., 2024) follow such a capability-oriented rule to construct domains. While preliminary steps in the data pipeline such as data cleaning, toxicity removal, quality filtering, and coreset selection are also important aspects, our work focuses on the subsequent challenge of weighting the given pre-curated, skill-specific domains.

Data mixing. Despite the widespread practice of domain-structured data curation in VLMs, the subsequent step of determining the proportional mixture of these domains largely relies on developer intuition or costly empirical tuning. For instance, LLaVA-One (Li et al., 2024a) and Flamingo (Alayrac et al., 2022) manually tuned domain weights for their promising performance. Other approaches, like that for LLaVA-NeXT (Liu et al., 2024b), involve reactively adding new data to address perceived skill gaps, which is inefficient and heuristic. InstructBLIP (Gu et al., 2024a) observes that ignoring the mixing problem in VLMs leads to unstable training and harms performance. While data mixing has been studied more formally for unimodal LLMs, these approaches are fundamentally ill-suited for VLMs. Most of them (Xie et al., 2023; Fan et al., 2024a; Liu et al., 2024c; Ye et al., 2024; Kang et al., 2024) rely on proxy models' training, which is difficult to combine in the multi-stage VLM pipeline. Recent directions (Xie et al., 2025; Zhang et al., 2025) integrate

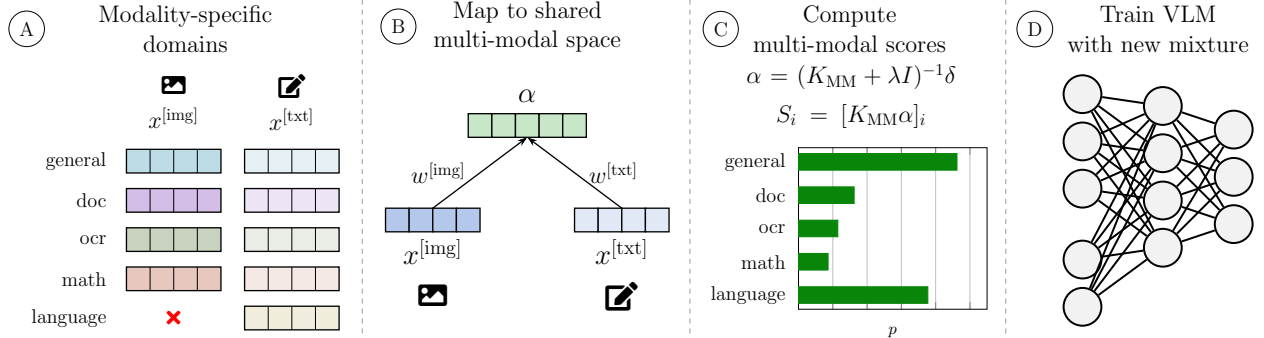


Figure 1: **Pipeline of multi-modal data mixing for VLM training.** ④ Modality-specific embeddings $x_i^{[v]}$ are extracted from the midstage trained model for each domain. Some domains may lack certain modalities (e.g., the language domain has no image data). ⑤ The k domains are then mapped to a shared multi-modal space by the coupling latent variables α of the multi-modal alignment objective (4). ⑥ The multi-modal kernel matrix K_{MM} is computed as the pairwise inner products between domain embeddings across modalities via (5). Finally, (6) is applied to K_{MM} and α to obtain score S_i , $i = 1, \dots, k$ indicating the multi-modal alignment of each domain. A resampling non-uniform distribution p is obtained by softmax-normalizing the scores. ⑦ Finally, image-text instruction tuning of the target VLM is carried out by sampling according to the obtained data mixture p .

into LLM training, but they are not designed to handle multimodal features and cannot manage domains with missing modalities.

3 Multi-modal Mixing with Modality-aware Domain Alignment

We propose **MaD-Mix**, a fusion-based framework for principled multi-modal data mixing. VLM training data presents unique challenges: feature heterogeneity and varying modality availability across domains. We address these by formulating mixing as measuring the projection of each domain onto a consensus direction. Section 3.1 derives the multi-modal objective by coupling domain contributions in a shared latent space. In Section 3.2, we extend this formulation to handle missing modalities explicitly. The practical mixing pipeline of **MaD-Mix** is shown in Figure 1.

Setup and objective. Let $\mathcal{D}_{\text{MM}} = \{D_i\}_{i \in [k]}$ be the set of k VLM training data domains (e.g., Math, OCR, etc.), where $[k]$ denotes the set of integers $\{1, \dots, k\}$. These domains define the target skill sets that the final trained VLM should possess. While samples within a domain D_i share the same modalities, the available modalities may vary across domains. Each sample $a^{[v]}$ from modality $v, v \in [V]$ (e.g., vision or text) can be represented through its semantic embedding $h^{(L)}(a^{[v]})$ extracted from the L -th hidden layer of the pretrained VLM h . The domain embedding $x_i^{[v]} \in \mathbb{R}^d$ for the v -th modality can be constructed as the semantic centroid $x_i^{[v]} = \frac{1}{|D_i|} \sum_{a^{[v]} \in D_i} h^{(L)}(a^{[v]})$, which can effectively represent data domains thanks to the high-dimensional, non-linear representations learned by Transformers (Xie et al., 2025; Ling et al., 2025). The data mixing objective is to determine a domain weight vector $p \in \Delta_k$ (Albalak et al., 2023; Fan et al., 2024a) for VLM training, where p_i serves as the sampling probability for domain D_i .

3.1 Multi-modal domain alignment scores

We first consider the single-modality setting. Given multiple domains representing various capabilities, the goal of VLM training is to learn generalizable representations that can transfer effectively across tasks. We seek a projection direction w in embedding space that captures the shared structure underlying all k domains. We define the alignment score S'_i of domain D_i as its projection onto this direction. This leads to the following primal optimization problem:

$$\min_{w, e} \frac{1}{2\lambda} \sum_{i=1}^k e_i^2 + \frac{1}{2} \|w\|_F^2 \quad \text{s.t. } e_i = 1 - w^\top x_i, i \in [k], \quad (1)$$

where $w \in \mathbb{R}^d$ represents the projection vector, $e = [e_1, \dots, e_k] \in \mathbb{R}^k$ denotes the individual projection errors for each domain, and $\lambda > 0$ is a regularization parameter. By assigning a uniform target value of 1 for all

domains, (1) drives the optimization to identify a consensus direction w that aligns with the entire collection of domain embeddings $\{x_i\}_{i \in [k]}$, rather than being skewed toward any specific one.

Remark 3.1 (Beamforming). The form (1) has a well-defined interpretation from signal processing. It is analogous to a *beamformer* (Van Trees, 2002) where the mean embedding acts as the desired steering vector and the covariance matrix represents the domain dispersion. The optimal projection corresponds to directions that balance maximizing the scores with the shared signal while minimizing interference through the covariance $(\Sigma + \lambda I_d)^{-1}$ operator. The resulting score $S'_i = w^\top x_i$ therefore quantifies how well each domain x_i captures the robust consensus direction.

To enable *multi-modal* integration, we reformulate the primal objective (1) into a dual-form lower bound, allowing multiple modalities to be aligned in a shared latent space. Through introducing latent variables α'_i and the Fenchel-Young inequality $\frac{1}{2\lambda}e^2 + \frac{\lambda}{2}\alpha'^2 \geq e\alpha'$, $\forall e, \alpha' \in \mathbb{R}^k$ (Rockafellar, 1974; Suykens, 2017), we can express the primal problem of single modality as:

$$\begin{aligned} J &= \frac{1}{2\lambda} \sum_{i=1}^k e_i^2 + \frac{1}{2} \|w\|_F^2 \quad \text{s.t. } e_i = 1 - w^\top x_i, i \in [k] \\ &\geq \sum_{i=1}^k e_i \alpha'_i - \frac{\lambda}{2} \|\alpha'\|_F^2 + \frac{1}{2} \|w\|_F^2 \\ &= \sum_{i=1}^k (1 - w^\top x_i) \alpha'_i - \frac{\lambda}{2} \|\alpha'\|_F^2 + \frac{1}{2} \|w\|_F^2 =: J_{\text{SM}}, \end{aligned} \quad (2)$$

where $\alpha' = [\alpha'_1, \dots, \alpha'_k] \in \mathbb{R}^k$ is the vector of latent variables. By analyzing the stationary conditions of the lower-bound single-modality objective function J_{SM} and eliminating the primal variable w , we obtain the following solution in the latent variables: $\alpha' = (K + \lambda I_k)^{-1} \mathbf{1}_k$, where $K \in \mathbb{R}^{k \times k}$ is the domain affinity kernel matrix defined by $K_{ij} = x_i^\top x_j$, and $I_k \in \mathbb{R}^{k \times k}$ and $\mathbf{1}_k \in \mathbb{R}^{k \times 1}$ denote the identity matrix and all-ones vector respectively. Then, the unimodal domain score S'_i can be expressed as: $S'_i = [K(K + \lambda I)^{-1} \mathbf{1}_k]_i$, which is consistent with the covariance-based solution derived from the original problem (1), with derivation details in Sections A.1 and A.2.

Importantly, such dual structure with explicit latent variables α'_i in (2) facilitates the extension to **multi-modal integration**. Let $w^{[v]}$ denote the projection weight for modality $v \in [V]$. Define the alignment objective for each modality v as $J_{\text{SM}}^{[v]}(w^{[v]}, \alpha)$. We express the multi-modal scoring objective as

$$\tilde{J}_{\text{MM}} = \sum_{v=1}^V J_{\text{SM}}^{[v]}(w^{[v]}, \alpha) = \sum_{v=1}^V \sum_{i=1}^k (1 - (w^{[v]})^\top x_i^{[v]}) \alpha_i - \frac{\lambda}{2} \sum_{v=1}^V \|\alpha\|_F^2 + \frac{1}{2} \sum_{v=1}^V \|w^{[v]}\|_F^2, \quad (3)$$

which implicitly sets $\alpha'^{[1]} = \dots = \alpha'^{[V]} = \alpha$, connecting domain embeddings across modalities in the shared latent space, thereby realizing *inter-modality couplings*.

Interpretation. The dual multi-modal objective (3) jointly optimizes the scores $(w^{[v]})^\top x_i^{[v]}$ for all domains and modalities. The first term of (3) can be interpreted as an energy function (Bengio et al., 2009) penalizing high-energy solutions, i.e., large $(1 - (w^{[v]})^\top x_i^{[v]})$ disagreements. The dual variable α_i serves as a consensus variable: large values push all modality weights to reduce disagreement for that domain. The remaining terms serve as regularization controlling the weight norm and the distribution of the dual variables.

3.2 Multi-modal scores with missing modalities

Accommodating data with incomplete modality coverage is a key challenge in VLM training. For instance, with vision and text modalities, some domains may only contain text, while others may present both. This scenario commonly occurs in practical settings as VLMs are typically trained on a mix of multi-modal and pure text data to retain the model's dialogue capabilities.

To address the issue of missing modalities, we adjust the projection errors appropriately. To be specific, we set $x_i^{[v]} = 0_d$ along with zero as the target for the missing modality v in the i -th domain, which ensures that

Algorithm 1 Multi-modal Data Mixtures (**MaD-Mix**)

- 1: **Input:** Number of domains k , number of modalities V , domain embeddings $x_i^{[v]} \in \mathbb{R}^d$ for available modalities, and regularization parameter λ .
- 2: Preprocessing: 1) Set $x_i^{[v]} = 0_d$ for missing modality v in domain i ; 2) Construct target vector $\delta \in \mathbb{R}^k$ where δ_i counts available modalities in domain i .
- 3: Modality kernels: $K^{[v]} = [(x_i^{[v]})^\top x_j^{[v]}]_{i,j=1}^k$.
- 4: Multi-modal domain affinity: $K_{\text{MM}} = \sum_{v=1}^V K^{[v]}$.
- 5: Alignment scores: $S_i^{[v]} = [K^{[v]}(K_{\text{MM}} + \lambda I)^{-1}\delta]_i$.
- 6: Domain weights: $p_i = \frac{\exp(\sum_{v=1}^V S_i^{[v]})}{\sum_{j=1}^k \exp(\sum_{v=1}^V S_j^{[v]})}$.
- 7: **Output:** Domain weights $p = [p_1, \dots, p_k]$.

domains lacking a modality do not contribute to the scoring objective. Incorporating the modality indicator $\delta_i^{[v]}$, the final multi-modal scoring objective from (3) can be expressed as:

$$J_{\text{MM}} = \sum_{v=1}^V \sum_{i=1}^k \left[(\delta_i^{[v]} - (w^{[v]})^\top x_i^{[v]})\alpha_i - \frac{\lambda}{2}\alpha_i^2 \right] + \frac{1}{2} \sum_{v=1}^V \|w^{[v]}\|_{\text{F}}^2, \quad (4)$$

where $\delta_i^{[v]} \in \{0, 1\}$ indicates the existence of modality v in domain D_i .

We obtain the solution in the shared latent variables α in the multi-modal setting by analyzing the stationary conditions of (4) through the derivation in Section A.3, summarized in the following Proposition.

Proposition 3.2 (Multi-modal scores). *Define the multi-modal kernel matrix as $K_{\text{MM}} \in \mathbb{R}^{k \times k}$ with entries $K_{\text{MM}ij} = \sum_{v=1}^V K_{ij}^{[v]}$, where $K_{ij}^{[v]} = (x_i^{[v]})^\top x_j^{[v]}$. The optimal latent variables for the multi-modal objective are given by:*

$$\alpha = (K_{\text{MM}} + \lambda I)^{-1}\delta, \quad (5)$$

where $\delta = [\delta_1, \dots, \delta_k]^\top$ with entries $\delta_i = \sum_{v=1}^V \delta_i^{[v]}$. Note that δ_i is always a positive constant since all domains have at least one modality. At optimality, the domain alignment score $S_i^{[v]} = w^{[v]^\top} x_i^{[v]}$ for modality v of domain D_i in kernel representation is:

$$S_i^{[v]} = [K^{[v]}(K_{\text{MM}} + \lambda I)^{-1}\delta]_i, \quad (6)$$

with K_{MM} realizing the modality couplings.

A high score $S_i^{[v]}$ indicates that the v -th modality of domain D_i has a large component along the cross-modal consensus direction expressed through multi-modal coupling coefficients α . To obtain the final domain distribution, we aggregate the scores $S_i^{[v]}$ across all modalities for each domain D_i . The resampling distribution p for VLM training is then obtained by softmax-normalizing the scores: $p_i = \frac{\exp(\sum_{v=1}^V S_i^{[v]})}{\sum_{j=1}^k \exp(\sum_{v=1}^V S_j^{[v]})}$.

Remark 3.3 (Spectral characterization). The multi-modal kernel matrix K_{MM} induces a spectral decomposition of the domain relationships. Let $K_{\text{MM}} = U\Sigma U^\top$ with eigenvalues $\{\sigma_j\}_{j=1}^k$ and eigenvectors $\{u_j\}_{j=1}^k$. In Section A.4, we show that the resulting score for domain D_i admits the expansion $S_i = \sum_{j=1}^k \frac{\sigma_j}{\sigma_j + \lambda} (u_j^\top \delta) (u_j)_i$. The **MaD-Mix** score applies a spectral soft-thresholding to the multi-modal kernel: directions associated with large eigenvalues (signal-dominated components) are preserved, and small-eigenvalue directions (noise-dominated components) are attenuated.

Computational complexity & practical implementation. Our algorithm is summarized in Algorithm 1. Computing embeddings $x_i^{[v]}$ requires a cheap inference pass through the model from the previous stage. The kernel score computation (6) is computationally cheap given the typically small number of domains k used in VLM training (detailed complexity analysis is given in Remark A.1). Notably, **MaD-Mix** operates independently of the VLM optimization procedure, enabling noninvasive integration into diverse pipelines by simply adjusting sampling weights. This approach is a key advantage in the VLM setting where many differing training pipelines are commonly used.

4 Experiments

We conduct a comprehensive empirical evaluation of our multi-modal data mixing method for visual instruction tuning of LLaVA-OneVision (Li et al., 2024a) across diverse VLM benchmarks. We follow the standard domain construction of (Li et al., 2024a), with each domain corresponding to a target VLM skill providing an ideal testbed for data mixing strategies (Laurençon et al., 2024; Dong et al., 2025). Furthermore, the data incorporate text, image, and video modalities and realistically reflect practical challenges such as the inconsistent availability of modalities across domains.

First, we evaluate our method on the stage-2 image-text instruction tuning (Li et al., 2024a), which contains five domains including text and image modalities, and compare average accuracy on multiple benchmarks to other mixing baselines. **MaD-Mix** accelerates training at expert-tuned performance with marginal computational cost. Further, we explore the transferability of our domain weights across model sizes and architectures on Qwen-VL. Then, we introduce an additional video modality, showing that our algorithmic mixing naturally extends to more complex multi-modal settings, yielding consistent improvements and providing an efficient, scalable alternative to costly expert tuning.

Training setup. We train LLaVA-OneVision 0.5B and 7B models with batch size 128, sequence length 8192, and learning rate 10^{-5} with cosine decay. In Section 4.1, models are trained for 4500 steps following Li et al. (2024a) s.t. each example is used only once. The training data consists of five domains: General, Doc/Chart/Screen, Math/Reasoning, General OCR, and Language. The first four domains are structured as image-text pairs, while the Language domain includes text data only, lacking the image modality. In Section 4.2, we introduce an additional VideoQA domain with video-text data and train for 3000 steps to further test our method’s multi-modal capabilities.

Baselines. UNIFORM is the cost-free mixture assigning equal weights $p_i = \frac{1}{k}$, which, despite its simplicity, can be a strong baseline (Michel et al., 2021; Fan et al., 2024a). HUMAN corresponds to the domain weights manually optimized by the authors of (Li et al., 2024a). TEXT, IMAGE, and VIDEO represent weights derived solving Equation (1) based on embeddings from a single modality. If a domain lacks a specific modality, its corresponding weight is set to zero. AVG averages the domain weights of all single modalities. For example, $\text{AVG} = \frac{1}{2}(\text{TEXT} + \text{IMAGE})$ in Section 4.1 and $\text{AVG} = \frac{1}{3}(\text{TEXT} + \text{IMAGE} + \text{VIDEO})$ in Section 4.2. Moreover, FUSED are the domain weights computed from the fused multi-modal embedding, which is generated by the VLM after processing all modalities as a unified sequence. **MaD-Mix** computes the domain weights through Equation (6). The processes of embedding extraction and domain weight assignment are detailed in Section B.3.

Evaluation benchmarks. We use various benchmarks for VLM evaluation in diverse tasks and they can be categorized into three classes following (Li et al., 2024a): (1) *Chart, Diagram, and Document Understanding*. Charts and diagrams are key formats for visual information expression. We evaluate on AI2D (Kembhavi et al., 2016), ChartQA (Masry et al., 2022), DocVQA (Mathew et al., 2021), and InfoVQA (Mathew et al., 2022), and OCRBench (Liu et al., 2024d) for text recognition. (2) *Perception and Multi-discipline Reasoning*. For more complex visual detection scenarios, we also evaluate on more challenging multi-disciplinary visual-language reasoning tasks. Specifically, we follow the multi-modal benchmarks of MME (Yin et al., 2023), MMBench (Liu et al., 2023b), and reasoning benchmarks including MathVerse (Zhang et al., 2024a), MMMU (Yue et al., 2024), and ScienceQA (Lu et al., 2022a). (3) *Real-world Understanding and Multi-modal Chatbots*. We also benchmark the capability of VLMs as a general-purpose assistant in the real world with specific benchmarks, including RealworldQA (x.ai, 2024) and MMStar (Chen et al., 2024b). In Table 4, we add two video benchmarks: Video-MMMU (Hu et al., 2025) and MVBench (Li et al., 2024b). We use the LLMs-Eval library (Zhang et al., 2024b) for evaluation.

4.1 MaD-Mix improves both 0.5B and 7B VLMs

We train LLaVA-OneVision-0.5B using the domain reweighting strategies discussed in Baselines above during the single-image (i.e., no video) training phase. The domain weights are visualized in Figure 2 (top) and listed in Section B.4. These models are evaluated on ten diverse benchmarks, presenting the 0-shot accuracy in Table 1. Our **MaD-Mix** achieves the highest average score across all benchmarks, bringing a 1.24% improvement over UNIFORM. Importantly, it even surpasses HUMAN that requires expensive and non-scalable grid searches on given domains, while our method can find mixtures with *negligible computational cost*. Remarkably, **MaD-Mix** learns faster: as shown in Figure 2 (bottom), it outperforms UNIFORM with just 56% steps and matches HUMAN with 78% steps, corresponding to $1.8\times$ and $1.28\times$ speedup factors, respectively.

For further analysis in Table 1, **MaD-Mix** outperforms 1) Avg that handles modalities independently, and 2) FUSED that uses the fused embeddings from VLM with all available modalities as input. Moreover, **MaD-Mix**

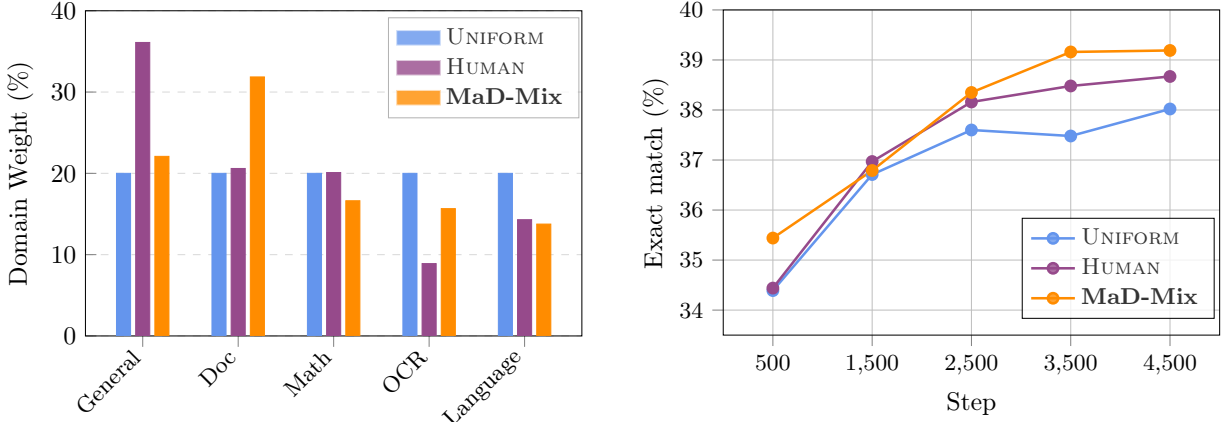


Figure 2: **Comparison of different data mixture strategies in the image-text instruction tuning.** (Left) Domain weights for UNIFORM, HUMAN, and MaD-Mix. (Right) Zero-shot average downstream accuracy of 0.5B models, where MaD-Mix achieves consistent improvement.

Table 1: **Comparison of data mixing strategies for LLaVA-0.5B image-text instruction tuning.** Results are reported as 0-shot accuracy across ten evaluation benchmarks. We compare our **MaD-Mix** against baselines: UNIFORM (equal weights), HUMAN (manual weights), AVG (averaged single-modality weights), and FUSED (weights from input concatenation).

Benchmark	UNIFORM	HUMAN	AVG	FUSED	MaD-Mix
AI2D	42.78 ± 0.04	43.75 ± 0.01	45.50 ± 0.02	44.59 ± 0.05	43.52 ± 0.09
DocVQA	42.90 ± 0.02	42.66 ± 0.00	42.44 ± 0.03	42.67 ± 0.01	42.92 ± 0.02
InfoVQA	22.25 ± 0.03	22.61 ± 0.07	22.43 ± 0.04	23.50 ± 0.03	22.13 ± 0.05
MathVerse	18.27 ± 0.03	17.26 ± 0.11	18.32 ± 0.06	19.29 ± 0.08	18.91 ± 0.07
MMBench	36.34 ± 0.00	40.21 ± 0.04	39.86 ± 0.08	37.71 ± 0.12	42.44 ± 0.04
MMStar	33.45 ± 0.06	36.04 ± 0.10	33.50 ± 0.14	34.44 ± 0.20	35.88 ± 0.03
MMMU	30.00 ± 0.16	29.67 ± 0.31	29.00 ± 0.09	29.22 ± 0.21	29.78 ± 0.16
ScienceQA	62.42 ± 0.02	65.84 ± 0.02	64.80 ± 0.04	63.46 ± 0.09	64.50 ± 0.01
OCRBench	45.30 ± 0.05	44.60 ± 0.09	45.30 ± 0.06	43.50 ± 0.09	45.80 ± 0.05
RealworldQA	46.27 ± 0.18	44.05 ± 0.06	45.49 ± 0.10	45.36 ± 0.12	46.54 ± 0.06
Average	38.00 ± 0.09	38.67 ± 0.12	38.66 ± 0.08	38.37 ± 0.12	39.24 ± 0.08
Number over UNIFORM	-	5/10	6/10	6/10	8/10

also surpasses unimodal strategies that ignore the information from other modalities, as demonstrated in Section B.5. This indicates the importance of distinctly considering the contributions of each modality and addressing the missing modal data specifically. Moreover, our ablation studies in Section B.6 demonstrate the robustness of **MaD-Mix**'s domain weights. We further ablate with an Orthogonal Score variant explicitly prioritizing feature dissimilarity, as shown in Section B.7. The observed results suggests that emphasizing domain heterogeneity alone is less effective in this setting than the signal captured by our score.

In addition, the downweighted domains do not result in sacrificing the model's corresponding capabilities. Specifically, although **MaD-Mix** downweights Math and OCR compared to UNIFORM, it preserves the capabilities on MathVerse and OCRBench in Table 1. This suggests that our method supports positive transfer across domains: *emphasizing a subset of high-score domains can promote emergent capabilities in others*, even if they receive less training weight.

Domain weights transfer to larger VLMs. Recent research on data mixing in text-only LLMs shows that domain weights derived from smaller models can be effectively transferred to larger ones (Xie et al., 2023; Fan et al., 2024a; Liu et al., 2024c). We investigate this phenomenon in VLMs by training 7B models

Table 3: **Transfer weights from LLaVA-0.5B to LLaVA-7B for image-text instruction tuning.** Results are reported as 0-shot accuracy across ten benchmarks. **MaD-Mix** improves performance on 8 out of 10 benchmarks over **UNIFORM**.

Benchmark	UNIFORM	HUMAN	AVG	FUSED	MaD-Mix
AI2D	74.48 ± 0.04	74.03 ± 0.11	75.10 ± 0.08	75.74 ± 0.05	75.58 ± 0.09
DocVQA	57.91 ± 0.08	58.64 ± 0.05	58.28 ± 0.12	57.29 ± 0.15	58.32 ± 0.03
InfoVQA	34.76 ± 0.15	35.91 ± 0.09	36.95 ± 0.07	36.06 ± 0.11	36.23 ± 0.18
MathVerse	29.31 ± 0.09	26.85 ± 0.14	27.33 ± 0.18	28.68 ± 0.06	28.55 ± 0.12
MMBench	75.69 ± 0.02	76.12 ± 0.03	76.23 ± 0.05	75.77 ± 0.08	75.74 ± 0.06
MMStar	49.04 ± 0.11	50.26 ± 0.16	50.44 ± 0.09	49.46 ± 0.14	50.19 ± 0.10
MMMU	46.33 ± 0.21	46.78 ± 0.18	46.78 ± 0.22	46.78 ± 0.17	46.89 ± 0.15
ScienceQA	87.31 ± 0.06	90.38 ± 0.02	89.53 ± 0.04	85.52 ± 0.09	90.23 ± 0.07
OCRBench	56.80 ± 0.13	57.30 ± 0.08	56.70 ± 0.11	56.60 ± 0.08	57.90 ± 0.14
RealworldQA	58.17 ± 0.10	57.91 ± 0.12	56.99 ± 0.14	57.65 ± 0.10	57.47 ± 0.05
Average	56.98 ± 0.11	57.42 ± 0.11	57.43 ± 0.13	56.96 ± 0.11	57.71 ± 0.11
Number over UNIFORM	-	7/10	7/10	5/10	8/10

with the domain weights obtained from 0.5B models. The evaluation results are presented in Table 3. Remarkably, **MaD-Mix** maintains its performance advantage over baselines even at this increased model scale, outperforming **UNIFORM** on 8 out of the 10 benchmarks.

Marginal computational cost. The computational complexity of our method is discussed in Section 3. In practice, (i) embedding extraction is a fast inference-only process. In our experiments, this step takes 35 minutes on a single H100 GPU. (ii) Alignment score computation via (6) completes in seconds since the number of domains is small. The cost of our weight computation is marginal compared to the 90 and 620 GPU hours required to train 0.5B and 7B VLMs, respectively. Our approach substantially reduces the need for expensive, time-consuming manual tuning of data mixtures, which is a key bottleneck in current VLM development.

Table 2: Computational cost is negligible relative to full model training. Cost in H100 GPU hours.

Component	Cost (h)
Embedding extraction	0.58
Score computation	0.01
Total	0.59
Training (0.5B)	90
Training (7B)	620

4.2 Scale to more complex tri-modal settings

We further demonstrate the flexibility of **MaD-Mix** in more complex multimodal scenarios by adding a VideoQA domain that introduces video–text data. This creates a total of six domains with three modalities: text, image, and video. Our domain weights for this new configuration are shown in Figure 3 (top) and fully reported in Section B.8. We train 0.5B and 7B models with new domain weights and evaluate models on both image-only benchmarks (same as Section 4.1) and two video benchmarks, MVBench (Li et al., 2024b) and Video-MMMU (Hu et al., 2025).

The results in Table 4 demonstrate that **MaD-Mix** maintains its superiority over **UNIFORM** in the more complex tri-modal setting. Notably, **MaD-Mix** matches **UNIFORM** performance in only 33% steps, as shown in Figure 3 (bottom), resulting in a 3 \times average speedup. In addition, **MaD-Mix** outperforms both **Avg** and **FUSED** on average. This validates the effectiveness of our multi-modal construction compared to single-modality mixtures and simple early fusion. Crucially, this experiment highlights the *extensibility* of our method to richer multi-modal configurations where manual expert-tuning becomes increasingly impractical.

Domain weights transfer to Qwen-VL-2B. To explore the cross-architecture transferability of **MaD-Mix**, we apply domain weights obtained from LLaVA-0.5B to Qwen-VL-2B (Wang et al., 2024) in this tri-modal setup. The results in Section B.10 show that **MaD-Mix** maintains its benefit compared with other baselines also on Qwen-VL-2B. This transferability suggests that **MaD-Mix** captures intrinsic data characteristics that generalize across architectures, indicating its potential utility for broader model development.

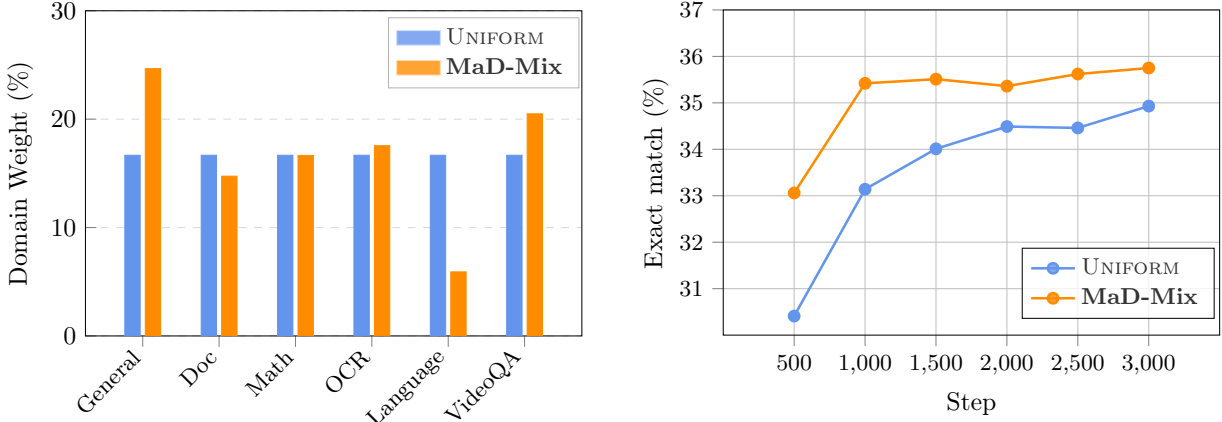


Figure 3: **Comparison of different data mixtures in the video-image-text instruction tuning.** (Left) Domain weights for **UNIFORM** and **MaD-Mix**. (Right) Zero-shot average downstream accuracy of 0.5B models, where **MaD-Mix** outperforms **UNIFORM** during the whole training process.

Table 4: **Comparison of data mixtures for LLaVA-0.5B/7B video-image-text instruction tuning.** Results are reported as 0-shot accuracy across twelve evaluation benchmarks. **MaD-Mix** achieves the best average performance on two model sizes. Results with standard deviations are in Section B.9.

Benchmark	0.5B				7B			
	UNIF.	AVG	FUSED	MaD-Mix	UNIF.	AVG	FUSED	MaD-Mix
AI2D	41.68	42.81	42.84	42.88	71.83	72.41	72.83	72.15
DocVQA	42.20	41.68	41.29	42.54	56.47	56.42	55.67	57.51
InfoVQA	21.65	21.97	21.17	22.40	35.74	34.65	34.40	35.89
MathVerse	15.61	15.62	17.77	15.10	25.63	25.52	24.75	26.40
MMBench	34.36	26.80	35.14	34.45	71.05	75.52	73.28	74.57
MMStar	30.43	35.54	36.14	33.97	48.18	49.03	46.55	48.79
MMMU	30.00	29.78	30.44	29.78	45.67	45.11	44.78	45.56
ScienceQA	60.29	60.29	59.40	61.03	83.44	86.07	83.29	87.26
OCRBench	45.30	43.20	46.60	45.00	56.50	56.90	57.60	57.20
RealworldQA	47.19	46.41	46.27	47.32	57.91	56.99	59.22	57.39
Video-MMMU	13.78	13.78	12.78	13.84	29.78	30.56	29.11	30.33
MVBench	36.67	36.50	37.02	40.70	52.73	51.58	53.12	53.60
Average	34.93	34.53	34.74	35.75	52.91	53.39	52.88	54.40
# over UNIF.	-	4/12	7/12	9/12	-	6/12	5/12	10/12

5 Conclusion

This paper presents a principled approach to the key problem of algorithmically determining sampling weights across pre-defined domains for vision-language model training with negligible additional computational cost. Our formulation through modality-aware fusion with coupling inter-modal variables addresses fundamental challenges in VLM training: handling missing modalities, learning cross-modal features, and determining domain weights without costly grid searches. Empirical evaluations demonstrate that our method improves training efficiency compared to both uniform and manually-tuned mixtures across diverse VLM benchmarks on average. Our approach allows direct integration with existing diverse VLM training pipelines and makes it valuable for practical applications, offering a path towards more data- and compute-efficient VLM training.

Acknowledgements

This work was supported by the Swiss National Science Foundation (SNSF) under grant numbers 2000-1-240094 and 200021_205011. This work was supported with project ID #37 as part of the Swiss AI Initiative, through a grant from the ETH Domain and computational resources provided by the Swiss National Supercomputing Centre (CSCS) under the Alps infrastructure. This work was supported by Hasler Foundation Program: Hasler Responsible AI (project number 21043). Research was sponsored by the Army Research Office and was accomplished under Grant Number W911NF-24-1-0048.

References

Jinze Bai, Shuai Bai, Shusheng Yang, Shijie Wang, Sinan Tan, Peng Wang, Junyang Lin, Chang Zhou, and Jingren Zhou. Qwen-vl: A versatile vision-language model for understanding, localization, text reading, and beyond. *arXiv preprint arXiv:2308.12966*, 2023a.

Haotian Liu, Chunyuan Li, Qingyang Wu, and Yong Jae Lee. Visual instruction tuning. *Advances in neural information processing systems*, 36, 2023a.

Bo Li, Yuanhan Zhang, Dong Guo, Renrui Zhang, Feng Li, Hao Zhang, Kaichen Zhang, Peiyuan Zhang, Yanwei Li, Ziwei Liu, et al. LLaVA-Onevision: Easy visual task transfer. *arXiv preprint arXiv:2408.03326*, 2024a.

Haotian Liu, Chunyuan Li, Yuheng Li, and Yong Jae Lee. Improved baselines with visual instruction tuning. In *Conference on Computer Vision and Pattern Recognition (CVPR)*, 2024a.

Jinze Bai, Shuai Bai, Yunfei Chu, Zeyu Cui, Kai Dang, Xiaodong Deng, Yang Fan, Wenbin Ge, Yu Han, Fei Huang, et al. Qwen technical report. *arXiv preprint arXiv:2309.16609*, 2023b.

An Yang, Anfeng Li, Baosong Yang, Beichen Zhang, Binyuan Hui, Bo Zheng, Bowen Yu, Chang Gao, Chengen Huang, Chenxu Lv, et al. Qwen3 technical report. *arXiv preprint arXiv:2505.09388*, 2025.

Abhimanyu Dubey, Abhinav Jauhri, Abhinav Pandey, Abhishek Kadian, Ahmad Al-Dahle, Aiesha Letman, Akhil Mathur, Alan Schelten, Amy Yang, Angela Fan, et al. The llama 3 herd of models. *arXiv e-prints*, pages arXiv-2407, 2024.

Gemini Team, Rohan Anil, Sebastian Borgeaud, Yonghui Wu, Jean-Baptiste Alayrac, Jiahui Yu, Radu Soricut, Johan Schalkwyk, Andrew M Dai, Anja Hauth, et al. Gemini: a family of highly capable multimodal models. *arXiv preprint arXiv:2312.11805*, 2023.

Wenliang Dai, Junnan Li, Dongxu Li, Anthony Tiong, Junqi Zhao, Weisheng Wang, Boyang Li, Pascale N Fung, and Steven Hoi. Instructblip: Towards general-purpose vision-language models with instruction tuning. *Advances in Neural Information Processing Systems (NeurIPS)*, 2023.

Bo Li, Yuanhan Zhang, Liangyu Chen, Jinghao Wang, Fanyi Pu, Joshua Adrian Cahyono, Jingkang Yang, Chunyuan Li, and Ziwei Liu. Otter: A multi-modal model with in-context instruction tuning. *IEEE Transactions on Pattern Analysis and Machine Intelligence*, 2025.

Peter Tong, Ellis Brown, Penghao Wu, Sanghyun Woo, Adithya Jairam Vedagiri IYER, Sai Charitha Akula, Shusheng Yang, Jihan Yang, Manoj Middepogu, Ziteng Wang, et al. Cambrian-1: A fully open, vision-centric exploration of multimodal LLMs. *Advances in Neural Information Processing Systems (NeurIPS)*, 2024.

Zhe Chen, Weiyun Wang, Yue Cao, Yangzhou Liu, Zhangwei Gao, Erfei Cui, Jinguo Zhu, Shenglong Ye, Hao Tian, Zhaoyang Liu, et al. Expanding performance boundaries of open-source multimodal models with model, data, and test-time scaling. *arXiv preprint arXiv:2412.05271*, 2024a.

Hugo Laurençon, Léo Tronchon, Matthieu Cord, and Victor Sanh. What matters when building vision-language models? *Advances in Neural Information Processing Systems (NeurIPS)*, 2024.

Haotian Liu, Chunyuan Li, Yuheng Li, Bo Li, Yuanhan Zhang, Sheng Shen, and Yong Jae Lee. LLaVA-NeXT: Improved reasoning, OCR, and world knowledge, January 2024b. URL <https://llava-vl.github.io/blog/2024-01-30-llava-next/>.

Samir Yitzhak Gadre, Gabriel Ilharco, Alex Fang, Jonathan Hayase, Georgios Smyrnis, Thao Nguyen, Ryan Marten, Mitchell Wortsman, Dhruba Ghosh, Jieyu Zhang, et al. Datacomp: In search of the next generation of multimodal datasets. *Advances in Neural Information Processing Systems (NeurIPS)*, 2023.

Jean-Baptiste Alayrac, Jeff Donahue, Pauline Luc, Antoine Miech, Iain Barr, Yana Hasson, Karel Lenc, Arthur Mensch, Katherine Millican, Malcolm Reynolds, et al. Flamingo: a visual language model for few-shot learning. *Advances in Neural Information Processing Systems (NeurIPS)*, 2022.

Sang Michael Xie, Hieu Pham, Xuanyi Dong, Nan Du, Hanxiao Liu, Yifeng Lu, Percy Liang, Quoc V. Le, Tengyu Ma, and Adams Wei Yu. DoReMi: Optimizing data mixtures speeds up language model pretraining. In *Advances in Neural Information Processing Systems (NeurIPS)*, 2023.

Simin Fan, Matteo Pagliardini, and Martin Jaggi. DOGE: Domain reweighting with generalization estimation. In *International Conference on Machine Learning (ICML)*, 2024a.

Qian Liu, Xiaosen Zheng, Niklas Muennighoff, Guangtao Zeng, Longxu Dou, Tianyu Pang, Jing Jiang, and Min Lin. Regmix: Data mixture as regression for language model pre-training. *arXiv preprint arXiv:2407.01492*, 2024c.

Feiyang Kang, Yifan Sun, Bingbing Wen, Si Chen, Dawn Song, Rafid Mahmood, and Ruoxi Jia. Autoscale: Automatic prediction of compute-optimal data composition for training llms. *arXiv preprint arXiv:2407.20177*, 2024.

Shuhao Gu, Jialing Zhang, Siyuan Zhou, Kevin Yu, Zhaohu Xing, Liangdong Wang, Zhou Cao, Jintao Jia, Zhuoyi Zhang, Yixuan Wang, et al. Infinity-mm: Scaling multimodal performance with large-scale and high-quality instruction data. *arXiv preprint arXiv:2410.18558*, 2024a.

Jiasheng Ye, Peiju Liu, Tianxiang Sun, Yunhua Zhou, Jun Zhan, and Xipeng Qiu. Data mixing laws: Optimizing data mixtures by predicting language modeling performance. *arXiv preprint arXiv:2403.16952*, 2024.

Wanyun Xie, Francesco Tonin, and Volkan Cevher. Chameleon: A flexible data-mixing framework for language model pretraining and finetuning. In *International Conference on Machine Learning (ICML)*, 2025.

Mozhi Zhang, Howe Tissue, Lu Wang, and Xipeng Qiu. Domain2vec: Vectorizing datasets to find the optimal data mixture without training. *International Conference on Machine Learning (ICML)*, 2025.

Zhenqing Ling, Daoyuan Chen, Liuyi Yao, Qianli Shen, Yaliang Li, and Ying Shen. Diversity as a reward: Fine-tuning llms on a mixture of domain-undetermined data. In *Advances in Neural Information Processing Systems (NeurIPS)*, 2025.

Alon Albalak, Liangming Pan, Colin Raffel, and William Yang Wang. Efficient online data mixing for language model pre-training. In *R0-FoMo: Robustness of Few-shot and Zero-shot Learning in Large Foundation Models Workshop*, 2023.

Harry L Van Trees. *Optimum array processing: Part IV of detection, estimation, and modulation theory*. John Wiley & Sons, 2002.

R Tyrrell Rockafellar. *Conjugate duality and optimization*. SIAM, 1974.

Johan AK Suykens. Deep restricted kernel machines using conjugate feature duality. *Neural computation*, 29(8):2123–2163, 2017.

Yoshua Bengio et al. Learning deep architectures for ai. *Foundations and trends® in Machine Learning*, 2(1):1–127, 2009.

Hongyuan Dong, Zijian Kang, Weijie Yin, Xiao Liang, Chao Feng, and Jiao Ran. Scalable vision language model training via high quality data curation. *arXiv preprint arXiv:2501.05952*, 2025.

Paul Michel, Sebastian Ruder, and Dani Yogatama. Balancing average and worst-case accuracy in multitask learning. *arXiv preprint arXiv:2110.05838*, 2021.

Aniruddha Kembhavi, Mike Salvato, Eric Kolve, Minjoon Seo, Hannaneh Hajishirzi, and Ali Farhadi. A diagram is worth a dozen images. In *Computer Vision–ECCV 2016: 14th European Conference, Amsterdam, The Netherlands, October 11–14, 2016, Proceedings, Part IV 14*, pages 235–251. Springer, 2016.

Ahmed Masry, Do Xuan Long, Jia Qing Tan, Shafiq Joty, and Enamul Hoque. Chartqa: A benchmark for question answering about charts with visual and logical reasoning. In *ACL*, 2022.

Minesh Mathew, Dimosthenis Karatzas, and CV Jawahar. Docvqa: A dataset for vqa on document images. In *WACV*, 2021.

Minesh Mathew, Viraj Bagal, Rubén Tito, Dimosthenis Karatzas, Ernest Valveny, and CV Jawahar. Info-graphicvqa. In *Proceedings of the IEEE/CVF Winter Conference on Applications of Computer Vision*, pages 1697–1706, 2022.

Yuliang Liu, Zhang Li, Mingxin Huang, Biao Yang, Wenwen Yu, Chunyuan Li, Xu-Cheng Yin, Cheng-Lin Liu, Lianwen Jin, and Xiang Bai. Ocrbench: on the hidden mystery of ocr in large multimodal models. *Science China Information Sciences*, 67(12):220102, 2024d.

Shukang Yin, Chaoyou Fu, Sirui Zhao, Ke Li, Xing Sun, Tong Xu, and Enhong Chen. A survey on multimodal large language models. *arXiv preprint arXiv:2306.13549*, 2023.

Yuan Liu, Haodong Duan, Yuanhan Zhang, Bo Li, Songyang Zhang, Wangbo Zhao, Yike Yuan, Jiaqi Wang, Conghui He, and Ziwei Liu. Mmbench: Is your multi-modal model an all-around player? *Technical Report*, 2023b.

Renrui Zhang, Dongzhi Jiang, Yichi Zhang, Haokun Lin, Ziyu Guo, Pengshuo Qiu, Aojun Zhou, Pan Lu, Kai-Wei Chang, Peng Gao, et al. Mathverse: Does your multi-modal llm truly see the diagrams in visual math problems? *arXiv preprint arXiv:2403.14624*, 2024a.

Xiang Yue, Yuansheng Ni, Kai Zhang, Tianyu Zheng, Ruoqi Liu, Ge Zhang, Samuel Stevens, Dongfu Jiang, Weiming Ren, and Yuxuan Sun. Mmmu: A massive multi-discipline multimodal understanding and reasoning benchmark for expert agi. In *CVPR*, 2024.

Pan Lu, Swaroop Mishra, Tony Xia, Liang Qiu, Kai-Wei Chang, Song-Chun Zhu, Oyvind Tafjord, Peter Clark, and Ashwin Kalyan. Learn to explain: Multimodal reasoning via thought chains for science question answering. In *The 36th Conference on Neural Information Processing Systems (NeurIPS)*, 2022a.

x.ai. Grok-1.5 vision preview, 2024. URL <https://x.ai/blog/grok-1.5v>.

Lin Chen, Jinsong Li, Xiaoyi Dong, Pan Zhang, Yuhang Zang, Zehui Chen, Haodong Duan, Jiaqi Wang, Yu Qiao, Dahua Lin, et al. Are we on the right way for evaluating large vision-language models? *arXiv preprint arXiv:2403.20330*, 2024b.

Kairui Hu, Penghao Wu, Fanyi Pu, Wang Xiao, Yuanhan Zhang, Xiang Yue, Bo Li, and Ziwei Liu. Video-mmmu: Evaluating knowledge acquisition from multi-discipline professional videos. *arXiv preprint arXiv:2501.13826*, 2025.

Kunchang Li, Yali Wang, Yinan He, Yizhuo Li, Yi Wang, Yi Liu, Zun Wang, Jilan Xu, Guo Chen, Ping Luo, et al. Mvbench: A comprehensive multi-modal video understanding benchmark. In *Proceedings of the IEEE/CVF Conference on Computer Vision and Pattern Recognition*, pages 22195–22206, 2024b.

Kaichen Zhang, Bo Li, Peiyuan Zhang, Fanyi Pu, Joshua Adrian Cahyono, Kairui Hu, Shuai Liu, Yuanhan Zhang, Jingkang Yang, Chunyuan Li, et al. Lmms-eval: Reality check on the evaluation of large multimodal models. *arXiv preprint arXiv:2407.12772*, 2024b.

Peng Wang, Shuai Bai, Sinan Tan, Shijie Wang, Zhihao Fan, Jinze Bai, Keqin Chen, Xuejing Liu, Jialin Wang, Wenbin Ge, Yang Fan, Kai Dang, Mengfei Du, Xuancheng Ren, Rui Men, Dayiheng Liu, Chang Zhou, Jingren Zhou, and Junyang Lin. Qwen2-vl: Enhancing vision-language model’s perception of the world at any resolution. *arXiv preprint arXiv:2409.12191*, 2024.

Lynn Houthuys, Rocco Langone, and Johan AK Suykens. Multi-view kernel spectral clustering. *Information Fusion*, 44:46–56, 2018.

Qinghua Tao, Francesco Tonin, Panagiotis Patrinos, and Johan AK Suykens. Tensor-based multi-view spectral clustering via shared latent space. *Information Fusion*, 108:102405, 2024.

Bo Li, Kaichen Zhang, Hao Zhang, Yuanhan Zhang, Renrui Zhang, and Feng Li. LLaVA-OneVision-Data. <https://huggingface.co/datasets/lmms-lab/LLaVA-OneVision-Data>, 2024c.

Francis Bach, Romain Thibaux, and Michael Jordan. Computing regularization paths for learning multiple kernels. *Advances in neural information processing systems*, 17, 2004.

Dustin Schwenk, Apoorv Khandelwal, Christopher Clark, Kenneth Marino, and Roozbeh Mottaghi. A-okvqa: A benchmark for visual question answering using world knowledge. In *European conference on computer vision*, pages 146–162. Springer, 2022.

Justin Johnson, Bharath Hariharan, Laurens Van Der Maaten, Li Fei-Fei, C Lawrence Zitnick, and Ross Girshick. Clevr: A diagnostic dataset for compositional language and elementary visual reasoning. In *Proceedings of the IEEE conference on computer vision and pattern recognition*, pages 2901–2910, 2017.

Douwe Kiela, Hamed Firooz, Aravind Mohan, Vedanuj Goswami, Amanpreet Singh, Pratik Ringshia, and Davide Testuggine. The hateful memes challenge: Detecting hate speech in multimodal memes. *Advances in neural information processing systems*, 33:2611–2624, 2020.

Renjie Pi, Jianshu Zhang, Jipeng Zhang, Rui Pan, Zhekai Chen, and Tong Zhang. Image textualization: An automatic framework for creating accurate and detailed image descriptions. *arXiv preprint arXiv:2406.07502*, 2024.

Pan Lu, Liang Qiu, Jiaqi Chen, Tony Xia, Yizhou Zhao, Wei Zhang, Zhou Yu, Xiaodan Liang, and Song-Chun Zhu. Iconqa: A new benchmark for abstract diagram understanding and visual language reasoning. *arXiv preprint arXiv:2110.13214*, 2021a.

Tanik Saikh, Tirthankar Ghosal, Amish Mittal, Asif Ekbal, and Pushpak Bhattacharyya. Scienceqa: A novel resource for question answering on scholarly articles. *International Journal on Digital Libraries*, 23(3):289–301, 2022.

Haiying Xia, Richeng Lan, Haisheng Li, and Shuxiang Song. St-vqa: shrinkage transformer with accurate alignment for visual question answering. *Applied Intelligence*, 53(18):20967–20978, 2023.

Manoj Acharya, Kushal Kafle, and Christopher Kanan. Tallyqa: Answering complex counting questions. In *Proceedings of the AAAI conference on artificial intelligence*, volume 33, pages 8076–8084, 2019.

Yiming Jia, Jiachen Li, Xiang Yue, Bo Li, Ping Nie, Kai Zou, and Wenhui Chen. Visualwebinstruct: Scaling up multimodal instruction data through web search. *arXiv preprint arXiv:2503.10582*, 2025.

Yuke Zhu, Oliver Groth, Michael Bernstein, and Li Fei-Fei. Visual7w: Grounded question answering in images. In *Proceedings of the IEEE conference on computer vision and pattern recognition*, pages 4995–5004, 2016.

Benny J Tang, Angie Boggust, and Arvind Satyanarayanan. Vistext: A benchmark for semantically rich chart captioning. *arXiv preprint arXiv:2307.05356*, 2023.

Danna Gurari, Qing Li, Abigale J Stangl, Anhong Guo, Chi Lin, Kristen Grauman, Jiebo Luo, and Jeffrey P Bigham. Vizwiz grand challenge: Answering visual questions from blind people. In *Proceedings of the IEEE conference on computer vision and pattern recognition*, pages 3608–3617, 2018.

Jason J Lau, Soumya Gayen, Asma Ben Abacha, and Dina Demner-Fushman. A dataset of clinically generated visual questions and answers about radiology images. *Scientific data*, 5(1):1–10, 2018.

Fangyu Liu, Guy Emerson, and Nigel Collier. Visual spatial reasoning. *Transactions of the Association for Computational Linguistics*, 11:635–651, 2023c.

Hugo Laurençon, Léo Tronchon, and Victor Sanh. Unlocking the conversion of web screenshots into html code with the websight dataset, 2024.

Guiming Hardy Chen, Shunian Chen, Ruifei Zhang, Junying Chen, Xiangbo Wu, Zhiyi Zhang, Zhihong Chen, Jianquan Li, Xiang Wan, and Benyou Wang. Allava: Harnessing gpt4v-synthesized data for lite vision-language models. *arXiv preprint arXiv:2402.11684*, 2024c.

Zhiyang Xu, Chao Feng, Rulin Shao, Trevor Ashby, Ying Shen, Di Jin, Yu Cheng, Qifan Wang, and Lifu Huang. Vision-flan: Scaling human-labeled tasks in visual instruction tuning. *arXiv preprint arXiv:2402.11690*, 2024a.

Pan Lu, Ran Gong, Shibiao Jiang, Liang Qiu, Siyuan Huang, Xiaodan Liang, and Song-Chun Zhu. Inter-gps: Interpretable geometry problem solving with formal language and symbolic reasoning. *arXiv preprint arXiv:2105.04165*, 2021b.

Yanzhe Zhang, Ruiyi Zhang, Jiuxiang Gu, Yufan Zhou, Nedim Lipka, Diyi Yang, and Tong Sun. Llavar: Enhanced visual instruction tuning for text-rich image understanding. *arXiv preprint arXiv:2306.17107*, 2023a.

Lin Chen, Jinsong Li, Xiaoyi Dong, Pan Zhang, Conghui He, Jiaqi Wang, Feng Zhao, and Dahua Lin. Sharegpt4v: Improving large multi-modal models with better captions. In *European Conference on Computer Vision*, pages 370–387. Springer, 2024d.

Shankar Kantharaj, Rixie Tiffany Ko Leong, Xiang Lin, Ahmed Masry, Megh Thakkar, Enamul Hoque, and Shafiq Joty. Chart-to-text: A large-scale benchmark for chart summarization. *arXiv preprint arXiv:2203.06486*, 2022.

Kushal Kafle, Brian Price, Scott Cohen, and Christopher Kanan. Dvqa: Understanding data visualizations via question answering. In *Proceedings of the IEEE conference on computer vision and pattern recognition*, pages 5648–5656, 2018.

Samira Ebrahimi Kahou, Vincent Michalski, Adam Atkinson, Ákos Kádár, Adam Trischler, and Yoshua Bengio. Figureqa: An annotated figure dataset for visual reasoning. *arXiv preprint arXiv:1710.07300*, 2017.

Zhoujun Cheng, Haoyu Dong, Zhiruo Wang, Ran Jia, Jiaqi Guo, Yan Gao, Shi Han, Jian-Guang Lou, and Dongmei Zhang. Hitab: A hierarchical table dataset for question answering and natural language generation. *arXiv preprint arXiv:2108.06712*, 2021.

Bryan Wang, Gang Li, Xin Zhou, Zhourong Chen, Tovi Grossman, and Yang Li. Screen2words: Automatic mobile ui summarization with multimodal learning. In *The 34th Annual ACM Symposium on User Interface Software and Technology*, pages 498–510, 2021.

Aniruddha Kembhavi, Minjoon Seo, Dustin Schwenk, Jonghyun Choi, Ali Farhadi, and Hannaneh Hajishirzi. Are you smarter than a sixth grader? textbook question answering for multimodal machine comprehension. In *Conference on Computer Vision and Pattern Recognition (CVPR)*, 2017.

Jiabo Ye, Anwen Hu, Haiyang Xu, Qinghao Ye, Ming Yan, Guohai Xu, Chenliang Li, Junfeng Tian, Qi Qian, Ji Zhang, et al. Ureader: Universal ocr-free visually-situated language understanding with multimodal large language model. *arXiv preprint arXiv:2310.05126*, 2023.

Akash Ghosh, B Venkata Sahith, Niloy Ganguly, Pawan Goyal, and Mayank Singh. How robust are the tabular qa models for scientific tables? a study using customized dataset. *arXiv preprint arXiv:2404.00401*, 2024.

Ryota Tanaka, Kyosuke Nishida, and Sen Yoshida. Visualmrc: Machine reading comprehension on document images. In *Proceedings of the AAAI Conference on Artificial Intelligence*, volume 35, pages 13878–13888, 2021.

Fuxiao Liu, Kevin Lin, Linjie Li, Jianfeng Wang, Yaser Yacoob, and Lijuan Wang. Aligning large multi-modal model with robust instruction tuning. *CoRR*, 2023d.

Shuaichen Chang, David Palzer, Jialin Li, Eric Fosler-Lussier, and Ningchuan Xiao. Mapqa: A dataset for question answering on choropleth maps. *arXiv preprint arXiv:2211.08545*, 2022.

Yilun Zhao, Yunxiang Li, Chenying Li, and Rui Zhang. Multihiertt: Numerical reasoning over multi hierarchical tabular and textual data. *arXiv preprint arXiv:2206.01347*, 2022.

Adam Dahlgren Lindström and Savitha Sam Abraham. Clevr-math: A dataset for compositional language, visual and mathematical reasoning. *arXiv preprint arXiv:2208.05358*, 2022.

Minjoon Seo, Hannaneh Hajishirzi, Ali Farhadi, Oren Etzioni, and Clint Malcolm. Solving geometry problems: Combining text and diagram interpretation. In *Proceedings of the 2015 conference on empirical methods in natural language processing*, pages 1466–1476, 2015.

Avinash Anand, Raj Jaiswal, Abhishek Dharmadhikari, Atharva Marathe, Harsh Popat, Harshil Mital, Ashwin R Nair, Kritarth Prasad, Sidharth Kumar, Astha Verma, et al. Geovqa: A comprehensive multimodal geometry dataset for secondary education. In *2024 IEEE 7th International Conference on Multimedia Information Processing and Retrieval (MIPR)*, pages 102–108. IEEE, 2024.

Zhuowan Li, Xingrui Wang, Elias Stengel-Eskin, Adam Kortylewski, Wufei Ma, Benjamin Van Durme, and Alan L Yuille. Super-clevr: A virtual benchmark to diagnose domain robustness in visual reasoning. In *Proceedings of the IEEE/CVF conference on computer vision and pattern recognition*, pages 14963–14973, 2023.

Pan Lu, Liang Qiu, Kai-Wei Chang, Ying Nian Wu, Song-Chun Zhu, Tanmay Rajpurohit, Peter Clark, and Ashwin Kalyan. Dynamic prompt learning via policy gradient for semi-structured mathematical reasoning. *arXiv preprint arXiv:2209.14610*, 2022b.

Jiaqi Chen, Tong Li, Jinghui Qin, Pan Lu, Liang Lin, Chongyu Chen, and Xiaodan Liang. Unigeo: Unifying geometry logical reasoning via reformulating mathematical expression. *arXiv preprint arXiv:2212.02746*, 2022.

Jiahui Gao, Renjie Pi, Jipeng Zhang, Jiacheng Ye, Wanjun Zhong, Yufei Wang, Lanqing Hong, Jianhua Han, Hang Xu, Zhenguo Li, et al. G-llava: Solving geometric problem with multi-modal large language model. *arXiv preprint arXiv:2312.11370*, 2023.

Mehran Kazemi, Hamidreza Alvari, Ankit Anand, Jialin Wu, Xi Chen, and Radu Soricut. Geomverse: A systematic evaluation of large models for geometric reasoning. *arXiv preprint arXiv:2312.12241*, 2023.

Renrui Zhang, Xinyu Wei, Dongzhi Jiang, Yichi Zhang, Ziyu Guo, Chengzhuo Tong, Jiaming Liu, Aojun Zhou, Bin Wei, Shanghang Zhang, et al. Mavis: Mathematical visual instruction tuning. *arXiv e-prints*, pages arXiv–2407, 2024c.

Chi Zhang, Feng Gao, Baoxiong Jia, Yixin Zhu, and Song-Chun Zhu. Raven: A dataset for relational and analogical visual reasoning. In *Proceedings of the IEEE/CVF conference on computer vision and pattern recognition*, pages 5317–5327, 2019.

Xiaoman Zhang, Chaoyi Wu, Ziheng Zhao, Weixiong Lin, Ya Zhang, Yanfeng Wang, and Weidi Xie. Pmc-vqa: Visual instruction tuning for medical visual question answering. *arXiv preprint arXiv:2305.10415*, 2023b.

Chris Wendler and H. Q. Gambot. RenderedText Dataset. <https://huggingface.co/datasets/wendlerc/RenderedText>, 2023.

Ye Yuan, Xiao Liu, Wondimu Dikubab, Hui Liu, Zhilong Ji, Zhongqin Wu, and Xiang Bai. Syntax-aware network for handwritten mathematical expression recognition. In *Proceedings of the IEEE/CVF conference on computer vision and pattern recognition*, pages 4553–4562, 2022.

U-V Marti and Horst Bunke. The iam-database: an english sentence database for offline handwriting recognition. *International journal on document analysis and recognition*, 5:39–46, 2002.

Anand Mishra, Kartikey Alahari, and CV Jawahar. Scene text recognition using higher order language priors. In *BMVC-British machine vision conference*. BMVA, 2012.

Oleksii Sidorov, Ronghang Hu, Marcus Rohrbach, and Amanpreet Singh. Textcaps: a dataset for image captioning with reading comprehension. In *Computer Vision–ECCV 2020: 16th European Conference, Glasgow, UK, August 23–28, 2020, Proceedings, Part II* 16, pages 742–758. Springer, 2020.

Amanpreet Singh, Guan Pang, Mandy Toh, Jing Huang, Wojciech Galuba, and Tal Hassner. Textocr: Towards large-scale end-to-end reasoning for arbitrary-shaped scene text. In *Proceedings of the IEEE/CVF conference on computer vision and pattern recognition*, pages 8802–8812, 2021.

Zhangchen Xu, Fengqing Jiang, Luyao Niu, Yuntian Deng, Radha Poovendran, Yejin Choi, and Bill Yuchen Lin. Magpie: Alignment data synthesis from scratch by prompting aligned llms with nothing. *arXiv preprint arXiv:2406.08464*, 2024b.

Yuanhan Zhang, Jinming Wu, Wei Li, Bo Li, Zeyun Ma, Ziwei Liu, and Chunyuan Li. Video instruction tuning with synthetic data. *arXiv preprint arXiv:2410.02713*, 2024d.

Zhou Yu, Dejing Xu, Jun Yu, Ting Yu, Zhou Zhao, Yuetong Zhuang, and Dacheng Tao. Activitynet-qa: A dataset for understanding complex web videos via question answering. In *AAAI Conference on Artificial Intelligence*, 2019.

Junbin Xiao, Xindi Shang, Angela Yao, and Tat-Seng Chua. Next-qa: Next phase of question-answering to explaining temporal actions. In *Conference on Computer Vision and Pattern Recognition (CVPR)*, 2021.

Viorica Pătrăucean, Lucas Smaira, Ankush Gupta, Adrià Recasens Continente, Larisa Markeeva, Dylan Banarse, Skanda Koppula, Joseph Heyward, Mateusz Malinowski, Yi Yang, Carl Doersch, Tatiana Matejovicova, Yury Sulsky, Antoine Miech, Alex Frechette, Hanna Klimczak, Raphael Koster, Junlin Zhang, Stephanie Winkler, Yusuf Aytar, Simon Osindero, Dima Damen, Andrew Zisserman, and João Carreira. Perception test: A diagnostic benchmark for multimodal video models. In *Advances in Neural Information Processing Systems (NeurIPS)*, 2023.

Tom B. Brown, Benjamin Mann, Nick Ryder, Melanie Subbiah, Jared Kaplan, Prafulla Dhariwal, Arvind Neelakantan, Pranav Shyam, Girish Sastry, Amanda Askell, Sandhini Agarwal, Ariel Herbert-Voss, Gretchen Krueger, Tom Henighan, Rewon Child, Aditya Ramesh, Daniel M. Ziegler, Jeffrey Wu, Clemens Winter, Christopher Hesse, Mark Chen, Eric Sigler, Mateusz Litwin, Scott Gray, Benjamin Chess, Jack Clark, Christopher Berner, Sam McCandlish, Alec Radford, Ilya Sutskever, and Dario Amodei. Language models are few-shot learners. In *Advances in Neural Information Processing Systems (NeurIPS)*, 2020.

Hugo Touvron, Louis Martin, Kevin Stone, Peter Albert, Amjad Almahairi, Yasmine Babaee, Nikolay Bashlykov, Soumya Batra, Prajjwal Bhargava, Shruti Bhosale, et al. Llama 2: Open foundation and fine-tuned chat models. *arXiv preprint arXiv:2307.09288*, 2023.

Cody Blakeney, Mansheej Paul, Brett W Larsen, Sean Owen, and Jonathan Frankle. Does your data spark joy? performance gains from domain upsampling at the end of training. *arXiv preprint arXiv:2406.03476*, 2024.

Alon Albalak, Yanai Lazar, Sang Michael Xie, Shayne Longpre, Nathan Lambert, Xinyi Wang, Niklas Muennighoff, Bairu Hou, Liangming Pan, Haewon Jeong, et al. A survey on data selection for language models. *arXiv preprint arXiv:2402.16827*, 2024.

Yiding Jiang, Allan Zhou, Zhili Feng, Sadhika Malladi, and J Zico Kolter. Adaptive data optimization: Dynamic sample selection with scaling laws. *arXiv preprint arXiv:2410.11820*, 2024.

Viraat Aryabumi, Yixuan Su, Raymond Ma, Adrien Morisot, Ivan Zhang, Acyr Locatelli, Marzieh Fadaee, Ahmet Üstün, and Sara Hooker. To code, or not to code? exploring impact of code in pre-training. *arXiv preprint arXiv:2408.10914*, 2024.

Shiori Sagawa, Pang Wei Koh, Tatsunori B Hashimoto, and Percy Liang. Distributionally robust neural networks for group shifts: On the importance of regularization for worst-case generalization. *International Conference on Learning Representations (ICLR)*, 2019.

Anvith Thudi and Chris J Maddison. Mixmax: Distributional robustness in function space via optimal data mixtures. *International Conference on Learning Representations (ICLR)*, 2024.

Simin Fan, David Grangier, and Pierre Ablin. Dynamic gradient alignment for online data mixing. *arXiv preprint arXiv:2410.02498*, 2024b.

Mayee F Chen, Michael Y Hu, Nicholas Lourie, Kyunghyun Cho, and Christopher Ré. Aioli: A unified optimization framework for language model data mixing. *arXiv preprint arXiv:2411.05735*, 2024e.

Mayee Chen, Nicholas Roberts, Kush Bhatia, Jue Wang, Ce Zhang, Frederic Sala, and Christopher Ré. Skill-it! a data-driven skills framework for understanding and training language models. *Advances in Neural Information Processing Systems*, 36:36000–36040, 2023.

Anvith Thudi, Eviannne Rovers, Yangjun Ruan, Tristan Thrush, and Chris J Maddison. Mixmin: Finding data mixtures via convex minimization. *arXiv preprint arXiv:2502.10510*, 2025.

William Held, Bhargavi Paranjape, Punit Singh Koura, Mike Lewis, Frank Zhang, and Todor Mihaylov. Optimizing pretraining data mixtures with llm-estimated utility. *arXiv preprint arXiv:2501.11747*, 2025.

Jared Kaplan, Sam McCandlish, Tom Henighan, Tom B Brown, Benjamin Chess, Rewon Child, Scott Gray, Alec Radford, Jeffrey Wu, and Dario Amodei. Scaling laws for neural language models. *arXiv preprint arXiv:2001.08361*, 2020.

Jordan Hoffmann, Sebastian Borgeaud, Arthur Mensch, Elena Buchatskaya, Trevor Cai, Eliza Rutherford, Diego de Las Casas, Lisa Anne Hendricks, Johannes Welbl, Aidan Clark, et al. Training compute-optimal large language models. *arXiv preprint arXiv:2203.15556*, 2022.

Haoran Que, Jiaheng Liu, Ge Zhang, Chenchen Zhang, Xingwei Qu, Yinghao Ma, Feiyu Duan, Zhiqi Bai, Jiakai Wang, Yuanxing Zhang, et al. D-cpt law: Domain-specific continual pre-training scaling law for large language models. *Advances in Neural Information Processing Systems*, 37:90318–90354, 2024.

Jiawei Gu, Zacc Yang, Chuanghao Ding, Rui Zhao, and Fei Tan. Cmr scaling law: Predicting critical mixture ratios for continual pre-training of language models. *arXiv preprint arXiv:2407.17467*, 2024b.

Muyang He, Yexin Liu, Boya Wu, Jianhao Yuan, Yueze Wang, Tiejun Huang, and Bo Zhao. Efficient multimodal learning from data-centric perspective. *arXiv preprint arXiv:2402.11530*, 2024.

Hu Xu, Saining Xie, Po-Yao Huang, Licheng Yu, Russell Howes, Gargi Ghosh, Luke Zettlemoyer, and Christoph Feichtenhofer. Cit: Curation in training for effective vision-language data. In *International Conference on Computer Vision (ICCV)*, 2023.

Anas Mahmoud, Mostafa Elhoushi, Amro Abbas, Yu Yang, Newsha Ardalani, Hugh Leather, and Ari S Morcos. Sieve: Multimodal dataset pruning using image captioning models. In *Conference on Computer Vision and Pattern Recognition (CVPR)*, 2024.

Tianyi Bai, Hao Liang, Binwang Wan, Yanran Xu, Xi Li, Shiyu Li, Ling Yang, Bozhou Li, Yifan Wang, Bin Cui, et al. A survey of multimodal large language model from a data-centric perspective. *arXiv preprint arXiv:2405.16640*, 2024.

Tadas Baltrušaitis, Chaitanya Ahuja, and Louis-Philippe Morency. Multimodal machine learning: A survey and taxonomy. *IEEE Transactions on Pattern Analysis and Machine Intelligence*, 41(2):423–443, 2019. doi: 10.1109/TPAMI.2018.2798607.

Renhao Huang, Hao Xue, Maurice Pagnucco, Flora Salim, and Yang Song. Multimodal trajectory prediction: A survey. *arXiv preprint arXiv:2302.10463*, 2023.

Lin Li, Guikun Chen, Hanrong Shi, Jun Xiao, and Long Chen. A survey on multimodal benchmarks: In the era of large ai models. *arXiv preprint arXiv:2409.18142*, 2024d.

George Barnum, Sabera Talukder, and Yisong Yue. On the benefits of early fusion in multimodal representation learning. *arXiv preprint arXiv:2011.07191*, 2020.

Said Yacine Boulahia, Abdenour Amamra, Mohamed Ridha Madi, and Said Daikh. Early, intermediate and late fusion strategies for robust deep learning-based multimodal action recognition. *Machine Vision and Applications*, 32(6):121, 2021.

Songtao Li and Hao Tang. Multimodal alignment and fusion: A survey. *arXiv preprint arXiv:2411.17040*, 2024.

Deyao Zhu, Jun Chen, Xiaoqian Shen, Xiang Li, and Mohamed Elhoseiny. Minigpt-4: Enhancing vision-language understanding with advanced large language models. In *The Twelfth International Conference on Learning Representations*, 2023.

Alec Radford, Jong Wook Kim, Chris Hallacy, Aditya Ramesh, Gabriel Goh, Sandhini Agarwal, Girish Sastry, Amanda Askell, Pamela Mishkin, Jack Clark, et al. Learning transferable visual models from natural language supervision. In *International conference on machine learning*, pages 8748–8763. PMLR, 2021.

Jiasen Lu, Dhruv Batra, Devi Parikh, and Stefan Lee. Vilbert: Pretraining task-agnostic visiolinguistic representations for vision-and-language tasks. *Advances in Neural Information Processing Systems (NeurIPS)*, 2019.

Zheng Cai, Maosong Cao, Haojong Chen, Kai Chen, Keyu Chen, Xin Chen, Xun Chen, Zehui Chen, Zhi Chen, Pei Chu, Xiaoyi Dong, Haodong Duan, Qi Fan, Zhaoye Fei, Yang Gao, Jiaye Ge, Chenya Gu, Yuzhe Gu, Tao Gui, Aijia Guo, Qipeng Guo, Conghui He, Yingfan Hu, Ting Huang, Tao Jiang, Penglong Jiao, Zhenjiang Jin, Zhikai Lei, Jiaxing Li, Jingwen Li, Linyang Li, Shuaibin Li, Wei Li, Yining Li, Hongwei Liu, Jiangning Liu, Jiawei Hong, Kaiwen Liu, Kuikun Liu, Xiaoran Liu, Chengqi Lv, Haijun Lv, Kai Lv, Li Ma, Runyuan Ma, Zerun Ma, Wenchang Ning, Linke Ouyang, Jiantao Qiu, Yuan Qu, Fukai Shang, Yunfan Shao, Demin Song, Zifan Song, Zhihao Sui, Peng Sun, Yu Sun, Huanze Tang, Bin Wang, Guoteng Wang, Jiaqi Wang, Jiayu Wang, Rui Wang, Yudong Wang, Ziyi Wang, Xingjian Wei, Qizhen Weng, Fan Wu, Yingtong Xiong, Chao Xu, Ruiliang Xu, Hang Yan, Yirong Yan, Xiaogui Yang, Haochen Ye, Huaiyuan Ying, Jia Yu, Jing Yu, Yuhang Zang, Chuyu Zhang, Li Zhang, Pan Zhang, Peng Zhang, Ruijie Zhang, Shuo Zhang, Songyang Zhang, Wenjian Zhang, Wenwei Zhang, Xingcheng Zhang, Xinyue Zhang, Hui Zhao, Qian Zhao, Xiaomeng Zhao, Fengzhe Zhou, Zaida Zhou, Jingming Zhuo, Yicheng Zou, Xipeng Qiu, Yu Qiao, and Dahu Lin. Internlm2 technical report. *arXiv preprint arXiv:2403.17297*, 2024.

A Problem formulation

A.1 Formulation for single modality setting

Let the data mixture problem consist of k data domains and their domain embeddings $x_i \in \mathbb{R}^d$ with their target $y_i \in \mathbb{R}$, $i = 1, \dots, k$. We first write the primal domain scoring problem for single modality:

$$\min_{w,e} \frac{1}{2\lambda} \sum_{i=1}^k e_i^2 + \frac{1}{2} \|w\|^2 \quad \text{s.t. } e_i = y_i - w^\top x_i, \quad i = 1, \dots, k, \quad (7)$$

where $w \in \mathbb{R}^d$, $e = [e_1, \dots, e_k] \in \mathbb{R}^k$ are the projections, $\lambda > 0$ is a regularization constant.

From the Lagrangian with dual variables ν :

$$\mathcal{L}(w, e; \nu) = \frac{1}{2\lambda} \sum_{i=1}^k e_i^2 + \frac{1}{2} \|w\|^2 - \sum_{i=1}^k \nu_i (e_i - y_i + w^\top x_i),$$

one takes the conditions for optimality, which are given as

$$\begin{cases} \frac{\partial \mathcal{L}}{\partial w} = w - \sum_{i=1}^k \nu_i x_i = 0 \implies w = \sum_{i=1}^k \nu_i x_i, \\ \frac{\partial \mathcal{L}}{\partial e_i} = \frac{1}{\lambda} e_i - \nu_i = 0 \implies e_i = \lambda \nu_i, \quad \forall i \\ \frac{\partial \mathcal{L}}{\partial \nu_i} = e_i - y_i + w^\top x_i = 0 \implies \lambda \nu_i - y_i + \sum_{j=1}^k \nu_j x_j^\top x_i = 0 \quad \forall i. \end{cases}$$

Eliminating w in the last condition gives the dual solution:

$$\begin{aligned} K\nu &= y - \lambda\nu, \\ (K + \lambda I)\nu &= y, \\ \nu &= (K + \lambda I)^{-1}y, \end{aligned}$$

where we defined the kernel matrix as $K = [x_i^\top x_j]_{i,j=1}^k$, and the target vector $y = [y_1, \dots, y_k]^\top$.

We are now ready to define the score of domain i as $S'_i = w^\top x_i$ in its kernel form:

$$S'_i = w^\top x_i = \left(\sum_{j=1}^k \nu_j x_j \right)^\top x_i = [K(K + \lambda I)^{-1}y]_i. \quad (8)$$

A.1.1 Primal and dual score representations

We can write Equation (7) in the unconstrained form:

$$\min_w \frac{1}{2\lambda} \sum_{i=1}^k (y_i - w^\top x_i)^2 + \frac{1}{2} \|w\|^2.$$

This is a ridge regression problem where the target vector is $y = [y_1, \dots, y_k]^\top$. Let X be the $k \times d$ data matrix with rows $x_1^\top, x_2^\top, \dots, x_k^\top$. Then the objective becomes:

$$\min_w \frac{1}{2\lambda} \|y - Xw\|^2 + \frac{1}{2} \|w\|^2.$$

The solution to this ridge regression problem is:

$$w = (X^\top X + \lambda I)^{-1} X^\top y.$$

The score for domain i is $S'_i = w^\top x_i$. The vector of scores can be computed as $S' = Xw$. Substituting the expression for w :

$$S'_i = [X(X^\top X + \lambda I)^{-1} X^\top y]_i.$$

This is equivalent to (8) by standard matrix identity, i.e., Woodbury identity. The following remark summarizes the computational aspect of the primal and dual representations of the score.

Remark A.1 (Efficient computation of the score). The primal solution is written in terms of the covariance $X^\top X$, while the dual solution is in terms of the kernel matrix XX^\top . In the context of data mixture with large VLMs, the embedding dimension d may be very large, so it is computationally advantageous to work in the dual with complexity $\mathcal{O}(k^3)$ where the number of data domains k is typically much smaller. We report the computational time of the defined score on a single A100 GPU in Table 5 as supporting evidence.

Table 5: Computational cost is negligible. Time on a single A100 GPU.

Number of Domains	Time (s)
10	0.07
100	0.09
1000	0.48
10000	21.85

A.2 Introducing latent variables

We first give a lower bound to the objective (7) and introduce latent variables α'_i , which will be used to couple the domains in the multi-modal setting. Starting from the primal single-modal problem (7), the following lower bound holds:

$$\begin{aligned} J &= \frac{1}{2\lambda} \sum_{i=1}^k e_i^2 + \frac{1}{2} \|w\|_F^2 \quad \text{s.t. } e_i = y_i - w^\top x_i, i = 1, \dots, k \\ &\geq \sum_{i=1}^k e_i \alpha'_i - \frac{\lambda}{2} \|\alpha'\|_F^2 + \frac{1}{2} \|w\|_F^2 \\ &= \sum_{i=1}^k (y_i - w^\top x_i) \alpha'_i - \frac{\lambda}{2} \|\alpha'\|_F^2 + \frac{1}{2} \|w\|_F^2 =: J_{\text{SM}}, \end{aligned}$$

where $\lambda > 0$ is a regularization constant and J_{SM} is the single modality objective. The above bound is based on the property that for two arbitrary vectors e, α' one has $\frac{1}{2\lambda} e^2 + \frac{\lambda}{2} \alpha'^2 \geq e \alpha'$, $\forall e, \alpha' \in \mathbb{R}^k$. The inequality can be verified using the Schur complement by writing in its quadratic form:

$$\frac{1}{2} \begin{bmatrix} e^T & \alpha'^\top \end{bmatrix} \begin{bmatrix} \frac{1}{\lambda} I & I \\ I & \lambda I \end{bmatrix} \begin{bmatrix} e \\ \alpha' \end{bmatrix} \geq 0.$$

From the Schur complement, it states the condition $\frac{1}{2}(\lambda I - I(\lambda I)I) \geq 0$, which proves the above inequality. This is also known as conjugate feature duality (Suykens, 2017) or the Fenchel–Young inequality for quadratic functions (Rockafellar, 1974).

Through the inequality, we have introduced latent variables, i.e. α'_i , into the objective. We proceed by studying the stationary condition of J_{SM} .

$$\begin{cases} \frac{\partial J_{\text{SM}}}{\partial w} = - \sum_{i=1}^k \alpha'_i x_i + w = 0 \quad \Rightarrow \quad w = \sum_{i=1}^k \alpha'_i x_i, \\ \frac{\partial J_{\text{SM}}}{\partial \alpha'_i} = y_i - w^\top x_i - \lambda \alpha'_i = 0 \quad \Rightarrow \quad \alpha'_i = \frac{1}{\lambda} (y_i - w^\top x_i) \quad \forall i. \end{cases} \quad (9)$$

By eliminating w in (9), we obtain

$$w^\top x_i = \left(\sum_{j=1}^k \alpha'_j x_j \right)^\top x_i = \sum_{j=1}^k \alpha'_j (x_j^\top x_i) \quad \forall i.$$

Thus the solution in the latent variables is

$$\begin{aligned} \alpha'_i &= \frac{1}{\lambda} \left(y_i - \sum_{j=1}^k \alpha'_j (x_j^\top x_i) \right) \\ \alpha' &= (K + \lambda I)^{-1} y. \end{aligned}$$

The score of domain i , i.e., $S_i = w^\top x_i$, writes in terms of the latent variables as:

$$S_i'' = w^\top x_i = \left(\sum_{j=1}^k \alpha'_j x_j \right)^\top x_i = \sum_{j=1}^k \alpha'_j (x_j^\top x_i) = [K(K + \lambda I)^{-1} y]_i,$$

which matches (8) obtained by the original problem (7). Let $y = 1_k$, it recovers the uni-modal score in Section 3.1.

A.3 Proof of Proposition 3.2

We first characterize the stationary points of J_{MM} defined in Equation (4), as the stationary conditions lead to the optimal solution in the dual of the multi-modal problem. Note that the coupling across modalities can be achieved by creating a common latent space (Houthuys et al., 2018; Tao et al., 2024), i.e., by introducing the same latent variables α across all modalities in J_{MM} . By taking the partial derivatives of the weights $w^{[v]}$ and the latent variables α , the conditions of the stationary points leading to MM scores are characterized by:

$$\left\{ \begin{array}{l} \frac{\partial J_{\text{MM}}}{\partial w^{[v]}} = - \sum_{i=1}^k \alpha_i x_i^{[v]} + w^{[v]} = 0 \implies w^{[v]} = \sum_{i=1}^k \alpha_i x_i^{[v]} \\ \frac{\partial J_{\text{MM}}}{\partial \alpha_i} = \sum_{v=1}^V \left(\delta_i^{[v]} - (w^{[v]})^\top x_i^{[v]} \right) - \lambda \alpha_i = 0 \\ \implies \sum_{v=1}^V \delta_i^{[v]} - \sum_{v=1}^V \left(\sum_{j=1}^k \alpha_j \underbrace{(x_j^{[v]})^\top x_i^{[v]}}_{K_{ij}^{[v]}} \right) - \lambda \alpha_i = 0 \\ \implies \sum_{v=1}^V \delta_i^{[v]} - \sum_{j=1}^k \alpha_j \sum_{v=1}^V K_{ij}^{[v]} - \lambda \alpha_i = 0 \\ \implies \sum_{v=1}^V \delta_i^{[v]} - \sum_{j=1}^k \alpha_j K_{\text{MM},ij} - \lambda \alpha_i = 0, \text{ where } K_{\text{MM},ij} = \sum_{v=1}^V K_{ij}^{[v]}. \end{array} \right.$$

Define the multi-modal kernel matrix as $K_{\text{MM}} \in \mathbb{R}^{k \times k}$ with entries $K_{\text{MM},ij} = \sum_{v=1}^V K_{ij}^{[v]}$, with $K_{ij}^{[v]} = (x_i^{[v]})^\top x_j^{[v]}$. The above conditions can be rewritten in matrix form as:

$$(K_{\text{MM}} + \lambda I)\alpha = \delta,$$

where $\delta \in \mathbb{R}^k$ is the vector with entries $\delta_i = \sum_{v=1}^V \delta_i^{[v]}$ with $\delta_i^{[v]} \in \{0, 1\}$ representing the existence of the modality v of the domain i . The solution in the latent variable therefore is

$$\alpha = (K_{\text{MM}} + \lambda I)^{-1} \delta.$$

We can compute the domain score for each modality as $S_i^{[v]} = w^{[v]^\top} x_i^{[v]}$. For modality v , at optimality:

$$w^{[v]} = \sum_{j=1}^k \alpha_j x_j^{[v]} \implies S_i^{[v]} = w^{[v]^\top} x_i^{[v]} = \sum_{j=1}^k \alpha_j (x_j^{[v]})^\top x_i^{[v]}.$$

Substituting $\alpha = (K_{\text{MM}} + \lambda I)^{-1} \delta$, it yields in matrix form:

$$S_i^{[v]} = \left[K^{[v]} (K_{\text{MM}} + \lambda I)^{-1} \delta \right]_i,$$

which is the multi-modal score of domain i for modality v . The ensemble score of domain i then considers all modalities as $S_i = \sum_{v=1}^V S_i^{[v]}$.

A.4 Eigendecomposition perspective

Alignment score functions as a robust steering direction. In fact, we can assert the following:

Lemma A.2. Let $K_{MM} \in \mathbb{R}^{k \times k}$ be the multi-modal kernel matrix with SVD $K_{MM} = U\Sigma U^\top$, where $U = [u_1, \dots, u_k]$ are the singular vectors and $\sigma_1 \geq \dots \geq \sigma_k$ are the singular values. The score S_i derived from the objective in Proposition 3.2 is given by: $S_i = \sum_{j=1}^k \left(\frac{\sigma_j}{\sigma_j + \lambda} \right) (u_j^\top \delta)(u_j)_i$.

Proof. By Proposition 3.2, the multi-modal score vector can be written as $S = K_{MM}(K_{MM} + \lambda I)^{-1}\delta$. Let $K_{MM} = U\Sigma U^\top$ be the eigendecomposition, where $U = [u_1, \dots, u_k]$ is orthonormal and $\Sigma = \text{diag}(\sigma_1, \dots, \sigma_k)$. Then $K_{MM}(K_{MM} + \lambda I)^{-1} = U\Sigma U^\top U(\Sigma + \lambda I)^{-1}U^\top = U\Sigma(\Sigma + \lambda I)^{-1}U^\top$, where $\Sigma(\Sigma + \lambda I)^{-1} = \text{diag}\left(\frac{\sigma_1}{\sigma_1 + \lambda}, \dots, \frac{\sigma_k}{\sigma_k + \lambda}\right)$. Writing $\delta = \sum_{j=1}^k (u_j^\top \delta) u_j$ in the eigenbasis of K_{MM} , we obtain $S = \sum_{j=1}^k \frac{\sigma_j}{\sigma_j + \lambda} (u_j^\top \delta) u_j$. Taking the i -th component yields $S_i = \sum_{j=1}^k \left(\frac{\sigma_j}{\sigma_j + \lambda} \right) (u_j^\top \delta)(u_j)_i$. \square

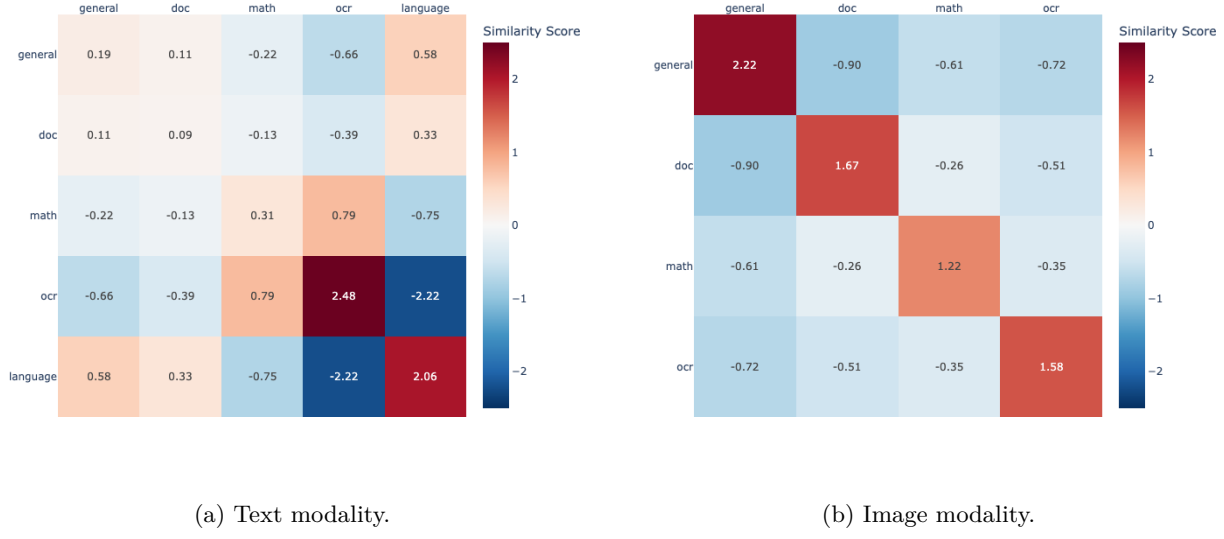
Therefore, our construction applies a spectral soft thresholding filter to the domain distribution. The associated operator dampens the noisy directions (small eigenvalues) and effectively measures the projection of domain i onto a robust semantic subspace (corresponding to large eigenvalues).

B Additional experiments

B.1 Difference between image and text modalities

In the multi-modality training process, there are two main challenges from the data perspective: (i) domains may have different modalities, and (ii) each domain's data features may vary significantly as captured by different modalities.

We take the LLaVA-OneVision dataset (Li et al., 2024c) as an example. The LLaVA-OneVision dataset includes five domains along with two modalities, image and text. Four domains include both image and text modalities, while the ‘‘Language’’ domain only has text. We visualize the embedding similarity matrix for text and image modalities independently in Figure 4. It shows that the domain relationships in different modalities can vary considerably, although the kernel magnitudes remain comparable. Note that the kernel matrices can be normalized to unit trace (Bach et al., 2004) if scales differed significantly.



(a) Text modality.

(b) Image modality.

Figure 4: Embedding kernel similarity matrix for different modalities.

B.2 Experimental setup

We use the LLaVA-OneVision publicly available data (Li et al., 2024c) for training and follow the domain segmentation in the LLaVA-OneVision paper (Li et al., 2024a). We use 3 seeds for the benchmark evaluations and report the standard deviations.

Note that some training datasets used in (Li et al., 2024a) were not released and some datasets use different naming conventions than (Li et al., 2024a). Our specific domain settings are:

- **General:** aokvqa (cauldron,llava_format) (Schwenk et al., 2022), clevr (cauldron,llava_format) (Johnson et al., 2017), hateful_memes (cauldron,llava_format) (Kiela et al., 2020), image_textualization (filtered) (Pi et al., 2024), iconqa (cauldron,llava_format) (Lu et al., 2021a), IconQA (MathV360K) (Lu et al., 2021a), scienceqa (cauldron,llava_format) (Saikh et al., 2022), scienceqa (nona_context) (Saikh et al., 2022), st_vqa (cauldron,llava_format) (Xia et al., 2023), tallyqa (cauldron,llava_format) (Acharya et al., 2019), VisualWebInstruct (filtered) (Jia et al., 2025), visual7w (cauldron,llava_format) (Zhu et al., 2016), vistext (cauldron) (Tang et al., 2023), VizWiz (MathV360K) (Gurari et al., 2018), vqarad (cauldron,llava_format) (Lau et al., 2018), vsr (cauldron,llava_format) (Liu et al., 2023c), websight (cauldron) (Laurençon et al., 2024), allava_instruct_laion4v (Chen et al., 2024c), allava_instruct_vflan4v (Chen et al., 2024c), vision_flan (filtered) (Xu et al., 2024a), intergps (cauldron,llava_format) (Lu et al., 2021b), llavar_gpt4_20k (Zhang et al., 2023a), sharegpt4o (Chen et al., 2024d), sharegpt4v (coco) (Chen et al., 2024d), sharegpt4v (knowledge) (Chen et al., 2024d), sharegpt4v (llava) (Chen et al., 2024d), sharegpt4v (sam) (Chen et al., 2024d)
- **Doc/Chart/Screen:** ai2d (cauldron,llava_format) (Kembhavi et al., 2016), ai2d (gpt4v) (Kembhavi et al., 2016), ai2d (internvl) (Kembhavi et al., 2016), chart2text (cauldron) (Kanthalraj et al., 2022), chartqa (cauldron,llava_format) (Masry et al., 2022), diagram_image_to_text (cauldron), dvqa (cauldron,llava_format) (Kafle et al., 2018), figureqa (cauldron,llava_format) (Kahou et al., 2017), hitab (cauldron,llava_format) (Cheng et al., 2021), infographic_vqa (Mathew et al., 2022), infographic_vqa_llava_format (Mathew et al., 2022), screen2words (cauldron) (Wang et al., 2021), tqa (cauldron,llava_format) (Kembhavi et al., 2017), ureader_cap (Ye et al., 2023), ureader_ie (Ye et al., 2023), robut_sqa (cauldron) (Ghosh et al., 2024), robut_wikisql (cauldron) (Ghosh et al., 2024), robut_wtq (cauldron,llava_format) (Ghosh et al., 2024), visualmrc (cauldron) (Tanaka et al., 2021), infographic (gpt4v) (Mathew et al., 2022), lrv_chart (Liu et al., 2023d), mapqa (cauldron,llava_format) (Chang et al., 2022), multihiertt (cauldron) (Zhao et al., 2022)
- **Math/Reasoning:** CLEVR-Math (MathV360K) (Lindström and Abraham, 2022), FigureQA (MathV360K) (Kahou et al., 2017), GEOS (MathV360K) (Seo et al., 2015), GeoQA+ (MathV360K) (Anand et al., 2024), Geometry3K (MathV360K) (Lu et al., 2021b), MapQA (MathV360K) (Chang et al., 2022), Super-CLEVR (MathV360K) (Li et al., 2023), TabMWP (MathV360K) (Lu et al., 2022b), UniGeo (MathV360K) (Chen et al., 2022), geo170k (align) (Gao et al., 2023), geo170k (qa) (Gao et al., 2023), geomverse (cauldron) (Kazemi et al., 2023), mavis_math_metagen (Zhang et al., 2024c), mavis_math_rule_geo (Zhang et al., 2024c), lrv_normal (filtered) (Liu et al., 2023d), geo3k (Lu et al., 2021b), raven (cauldron) (Zhang et al., 2019), PMC-VQA (MathV360K) (Zhang et al., 2023b), tabmwp (cauldron) (Lu et al., 2022b)
- **General OCR:** chrome_writting (Wendler and Gambot, 2023), hme100k (Yuan et al., 2022), iam (cauldron) (Marti and Bunke, 2002), iiit5k (Mishra et al., 2012), k12_printing, rendered_text (cauldron) (Wendler and Gambot, 2023), textcaps (Sidorov et al., 2020), textocr (gpt4v) (Singh et al., 2021), sroie, orand_car_a
- **Language:** magpie_pro (l3_80b_mt), magpie_pro (l3_80b_st), magpie_pro (qwen2_72b_st) (Xu et al., 2024b)
- **Video:** academic_qa, youtube (Zhang et al., 2024d), ActivityNetQA (Yu et al., 2019), NeXT-QA Xiao et al. (2021), PerceptionTest (Pătrăucean et al., 2023)

B.3 Embedding extraction and domain weight assignment

For embedding computation, we use the pretrained LLaVA-OneVision model that has completed stage-1.5 pre-training and we randomly sample a subset of data from each domain. Given the presence of multiple datasets per domain, we extracted embeddings for 512 samples from each individual dataset. These sample embeddings were then averaged to create a single representation for each dataset. Subsequently, we averaged these dataset-level embeddings to capture the overall character of its respective domain. Then, we use domain-level embeddings to compute domain weights.

Once we compute the domain weights p_i using Algorithm 1, our training sampling strategy takes dataset size into account as follows. We sample datasets proportionally to their size within each domain, and then sample individual data points uniformly from the chosen dataset. This results in the final sampling probability for a dataset DS in domain D_i being $P = \frac{|DS|}{|D_i|} p_i$, followed by uniformly sampling over instances in DS .

B.4 Domain weights for the image-text instruction tuning (Section 4.1)

We report domain weights for Section 4.1 with five domains and two modalities in Table 6. Note that $\text{AVG} = \frac{1}{2} (\text{TEXT} + \text{IMAGE})$. IMAGE^\dagger sets its Language weight as same as HUMAN and reweight the others in IMAGE.

B.5 Performance of domain weights computed by single modality

We add two unimodal strategies, TEXT and IMAGE † , in Tables 7 and 8 as addition for Tables 1 and 3. These two unimodal methods compute the domain weights derived from single modality in Section 3.1, based solely on text or image embeddings. Note that the Language domain does not have image data, thus IMAGE has

Table 6: **VLM Mixtures for the image-text instruction tuning.** Domain weights of different mixing strategies. IMAGE^\dagger sets its Language weight as same as HUMAN and reweight the others in IMAGE.

Domain	UNI.	HUMAN	TEXT	IMAGE	AVG	FUSED	MaD-Mix	IMAGE †
General	20.00	36.10	20.90	35.66	28.28	14.74	22.09	30.56
Doc/Chart/Screen	20.00	20.60	43.28	29.49	36.29	40.95	31.86	25.27
Math/Reasoning	20.00	20.10	15.24	17.92	16.58	20.21	16.63	15.36
General OCR	20.00	8.90	10.22	16.93	13.58	14.14	15.66	14.51
Language	20.00	14.30	10.35	0.00	5.18	9.95	13.76	14.30

0% on this domain. For a more reasonable comparison, we set its Language domain weight to the same as HUMAN and reweight the others, finalizing to IMAGE^\dagger in Table 6. Importantly, **MaD-Mix** still outperforms these unimodal strategies.

Table 7: **Comparison of data mixing strategies for LLaVA-0.5B image-text instruction tuning.** Results are reported as 0-shot accuracy across ten evaluation benchmarks. **MaD-Mix** achieves the best average performance, including the single-modality methods.

Benchmark	UNIFORM	HUMAN	AVG	FUSED	MaD-Mix	TEXT	IMAGE †
AI2D	42.78	43.75	45.50	44.59	43.52	45.95	44.33
DocVQA	42.90	42.66	42.44	42.67	42.92	43.08	42.42
InfoVQA	22.25	22.61	22.43	23.50	22.13	23.45	21.47
MathVerse	18.27	17.26	18.32	19.29	18.91	16.50	18.53
MMBench	36.34	40.21	39.86	37.71	42.44	35.82	39.00
MMStar	33.45	36.04	33.50	34.44	35.88	34.19	34.67
MMMU	30.00	29.67	29.00	29.22	29.78	27.89	30.67
ScienceQA	62.42	65.84	64.80	63.46	64.50	64.60	63.86
OCRBench	45.30	44.60	45.30	43.50	45.80	45.30	45.20
RealworldQA	46.27	44.05	45.49	45.36	46.54	45.36	46.67
Average	38.00	38.67	38.66	38.37	39.24	38.21	38.69
# over UNIFORM	-	5/10	6/10	6/10	8/10	5/10	7/10

Table 8: **Comparison of data mixing strategies for LLaVA-7B image-text instruction tuning.** Results are reported as 0-shot accuracy across ten evaluation benchmarks. **MaD-Mix** achieves the best average performance, including single-modality methods.

Benchmark	UNIFORM	HUMAN	AVG	FUSED	MaD-Mix	TEXT	IMAGE †
AI2D	74.48	74.03	75.10	75.74	75.58	75.42	75.58
DocVQA	57.91	58.64	58.28	57.29	58.32	58.73	57.86
InfoVQA	34.76	35.91	36.95	36.06	36.23	36.83	36.22
MathVerse	29.31	26.85	27.33	28.68	28.55	26.14	27.83
MMBench	75.69	76.12	76.23	75.77	75.74	75.60	76.98
MMStar	49.04	50.26	50.44	49.46	50.19	49.51	50.72
MMMU	46.33	46.78	46.78	46.78	46.89	47.11	45.67
ScienceQA	87.31	90.38	89.53	85.52	90.23	86.91	90.08
OCRBench	56.80	57.30	56.70	56.60	57.90	57.70	57.50
RealworldQA	58.17	57.91	56.99	57.65	57.47	57.65	57.39
Average	56.98	57.42	57.43	56.96	57.71	57.16	57.59
# over UNIFORM	-	7/10	7/10	5/10	8/10	6/10	6/10

B.6 Ablation studies

Regularization parameter λ . The parameter λ is related to the degree of regularization. Despite this control, Table 9 demonstrates that our obtained domain weights are largely stable with respect to changes in λ .

Number of samples for embedding extraction. As we discussed in Section B.3, we sample a subset of datasets for embedding extraction. We test the robustness of domain weights with respect to the number of samples. The domain weights based on 256, 512, or 1024 samples from each individual dataset are reported in Table 9, which confirms that the domain weights obtained are stable regardless of the number of samples.

Embedding aggregation. Except for averaging the dataset-level averaged embeddings to represent each domain, another way is to aggregate dataset-level embeddings to domain embeddings according to their dataset sizes. Basically, sum the dataset-level embeddings reweighted by their sizes as domain weights. The domain weights computed by these two strategies are highly similar, as reported in Table 9.

Model sizes. We use the domain weights obtained from the LLaVA-0.5B model’s embeddings and test the transferability for LLaVA-7B shown in Table 3. We compute domain weights based on the embeddings from LLaVA-7B as well. The result reported in Table 9 demonstrates that domain weights are stable across model sizes.

The number of training steps for the pretrained model. Regarding the sufficiency of feature extraction, the latent representations are from the mid-stage checkpoint of LLaVA-OneVision (Li et al., 2024a), which is a well-trained model. We additionally conducted a stability analysis by continuing training this checkpoint on its public mid-training data for 500 and 1000 additional steps and recomputed domain weights using our method. The results, presented in Table 9, demonstrate that the domain weights remain stable throughout training.

Number of domains. We run additional experiments with a reduced number of domains. We exclude ‘General’ from the original five domains, and the new domain weights obtained by **MaD-Mix** are: 26.7% Doc/Chart/Screen, 28.7% Math/Reasoning, 31.6% General OCR, and 13.0% Language. The domain weights of UNIFORM are 25% per domain. Table 10 demonstrates that **MaD-Mix** consistently shows a higher average accuracy. This validates the robustness of our method across different numbers of domains. Furthermore, the experiment in Section 4.2, which introduces a Video domain, demonstrates that **MaD-Mix** remains effective as the number of domains changes.

Table 9: **Domain weights across λ values, number of samples, model sizes, and the number of steps for pretrained checkpoints.** Our method is robust to the choice of λ , the number of samples used, embedding aggregation methods, model sizes and the number of steps.

Domain	λ Values			Number of Samples			Aggregate embeddings	
	1	10	100	256	512	1024	Equally	Dataset sizes
General	21.57	22.09	23.14	24.48	22.09	23.96	22.09	23.20
Doc/Chart/Screen	28.90	31.86	34.79	27.32	31.86	30.84	31.86	30.98
Math/Reasoning	17.47	16.63	15.95	18.71	16.63	17.32	16.63	17.80
General OCR	16.74	15.66	14.49	16.72	15.66	17.04	15.66	16.91
Language	15.32	13.76	11.64	12.77	13.76	10.84	13.76	11.11

Domain	Model sizes		# training steps for pretrained model		
	0.5B	7B	Pretrained model	+500 steps	+1000 steps
General	22.09	21.15	22.09	21.65	22.59
Doc/Chart/Screen	31.86	29.91	31.86	30.12	29.96
Math/Reasoning	16.63	19.64	16.63	18.74	18.82
General OCR	15.66	17.06	15.66	15.17	15.82
Language	13.76	12.23	13.76	14.33	12.99

B.7 Alignment score vs Orthogonal score

To further ablate the benefit introduced in Section 3, we introduce the ‘‘Orthogonal Score’’ to quantify the uniqueness of different domains, i.e., downweighting high-alignment domains. Specifically for the domain j , set $e_i = \gamma_i - w^\top x_i$, with $\gamma_i = 1$ if $i = j$, 0 otherwise in Equation (1). And Equation (4) becomes

$$J_{\text{MM}}^{\text{orth}} = \sum_{v=1}^V \sum_{i=1}^k \left[(\delta_i^{[v]} \gamma_i - (w^{[v]})^\top x_i^{[v]}) \alpha_i - \frac{\lambda}{2} \alpha_i^2 \right] + \frac{1}{2} \sum_{v=1}^V \|w^{[v]}\|_F^2.$$

The orthogonal score derived by this new objective is

$$S_j^{[v]} = \delta_j \left[K^{[v]} (K_{\text{MM}} + \lambda I)^{-1} \right]_{jj}.$$

Table 10: **Comparison of data mixtures on 4 domains for LLaVA-0.5B image-text instruction tuning.** **MaD-Mix** is robust across different numbers of domains.

Benchmark	UNIFORM	MaD-Mix
AI2D	42.75	43.75
DocVQA	40.79	41.71
InfoVQA	22.89	22.96
MathVerse	17.51	18.27
MMBench	30.76	33.59
MMStar	35.68	33.24
MMU	28.89	31.78
ScienceQA	53.99	54.09
OCRBench	43.30	44.70
RealworldQA	38.30	42.88
Average	35.48	36.69
Number over UNIFORM	-	9/10

We report the downstream performance of domain weights computed through Orthogonal score in Table 11. For comparison, we also present the original scores used in our method (**MaD-Mix**) below. The performance of **MaD-Mix** shows higher average accuracy than Orthogonal score. Importantly, Orthogonal score performs worse than UNIFORM on average (37.62 vs 38.00).

Table 11: **Comparison of Orthogonal and Alignment scores for LLaVA-0.5B image-text instruction tuning.** Orthogonal score is even worse than UNIFORM (37.62 vs 38.00).

Benchmark	Orthogonal score	Alignment score (MaD-Mix)
AI2D	43.04	43.52
DocVQA	41.58	42.92
InfoVQA	21.49	22.13
MathVerse	15.99	18.91
MMBench	32.65	42.44
MMStar	34.52	35.88
MMU	30.22	29.78
ScienceQA	64.25	64.50
OCRBench	46.30	45.80
RealworldQA	46.14	46.54
Average	37.62	39.24

B.8 Domain weights for video-image-text instruction tuning (Section 4.2)

We report domain weights for Section 4.2 with six domains and three modalities in Table 12. Note that AVG = $\frac{1}{3}$ (TEXT+IMAGE+VIDEO).

Table 12: **VLM Mixtures.** Domain weights across different mixing strategies for three modalities.

Domain	UNIFORM	TEXT	IMAGE	VIDEO	AVG	FUSED	MaD-Mix
General	16.67	16.62	35.66	0.00	17.43	10.77	24.66
Doc/Chart/Screen	16.67	14.42	29.49	0.00	16.70	13.20	14.74
Math/Reasoning	16.67	30.73	17.92	0.00	16.22	9.44	16.65
General OCR	16.67	9.27	16.93	0.00	8.73	38.60	17.55
Language	16.67	13.89	0.00	0.00	4.63	16.73	5.91
Video	16.67	15.08	0.00	100.00	38.36	11.26	20.49

B.9 Table 4 with standard deviations

We show the results with standard deviations of Table 4 in Tables 13 and 14.

Table 13: Comparison of data mixtures for LLaVA-0.5B video-image-text instruction tuning.

Benchmark	UNIFORM	AVG	FUSED	MaD-Mix
AI2D	41.68 ± 0.08	42.81 ± 0.09	42.84 ± 0.10	42.88 ± 0.04
DocVQA	42.20 ± 0.06	41.68 ± 0.05	41.29 ± 0.06	42.54 ± 0.08
InfoVQA	21.65 ± 0.07	21.97 ± 0.06	21.17 ± 0.08	22.40 ± 0.10
MathVerse	15.61 ± 0.10	15.62 ± 0.14	17.77 ± 0.11	15.10 ± 0.08
MMBench	34.36 ± 0.02	26.80 ± 0.03	35.14 ± 0.06	34.45 ± 0.04
MMStar	30.43 ± 0.05	35.54 ± 0.08	36.14 ± 0.06	33.97 ± 0.04
MMMU	30.00 ± 0.15	29.78 ± 0.09	30.44 ± 0.13	29.78 ± 0.11
ScienceQA	60.29 ± 0.11	60.29 ± 0.10	59.40 ± 0.12	61.03 ± 0.09
OCRbench	45.30 ± 0.12	43.20 ± 0.07	46.60 ± 0.08	45.00 ± 0.15
RealworldQA	47.19 ± 0.18	46.41 ± 0.16	46.27 ± 0.12	47.32 ± 0.10
Video-MMMU	13.78 ± 0.08	13.78 ± 0.04	12.78 ± 0.10	13.84 ± 0.06
MVBench	36.67 ± 0.06	36.50 ± 0.10	37.02 ± 0.10	40.70 ± 0.12
Average	34.93 ± 0.10	34.53 ± 0.09	34.74 ± 0.10	35.75 ± 0.09
Number over UNIFORM	-	$4/12$	$7/12$	$9/12$

Table 14: Comparison of data mixtures for LLaVA-7B video-image-text instruction tuning.

Benchmark	UNIFORM	AVG	FUSED	MaD-Mix
AI2D	71.83 ± 0.03	72.41 ± 0.08	72.83 ± 0.06	72.15 ± 0.06
DocVQA	56.47 ± 0.04	56.42 ± 0.06	55.67 ± 0.08	57.51 ± 0.10
InfoVQA	35.74 ± 0.12	34.65 ± 0.10	34.40 ± 0.07	35.89 ± 0.06
MathVerse	25.63 ± 0.11	25.52 ± 0.12	24.75 ± 0.08	26.40 ± 0.14
MMBench	71.05 ± 0.03	75.52 ± 0.06	73.28 ± 0.04	74.57 ± 0.05
MMStar	48.18 ± 0.08	49.03 ± 0.06	46.55 ± 0.04	48.79 ± 0.07
MMMU	45.67 ± 0.14	45.11 ± 0.10	44.78 ± 0.12	45.56 ± 0.13
ScienceQA	83.44 ± 0.04	86.07 ± 0.13	83.29 ± 0.10	87.26 ± 0.08
OCRbench	56.50 ± 0.11	56.90 ± 0.08	57.60 ± 0.09	57.20 ± 0.14
RealworldQA	57.91 ± 0.16	56.99 ± 0.15	59.22 ± 0.08	57.39 ± 0.09
Video-MMMU	29.78 ± 0.07	30.56 ± 0.05	29.11 ± 0.08	30.33 ± 0.06
MVBench	52.73 ± 0.08	51.58 ± 0.12	53.12 ± 0.07	53.60 ± 0.11
Average	52.91 ± 0.09	53.39 ± 0.10	52.88 ± 0.08	54.40 ± 0.10
Number over UNIFORM	-	$6/12$	$5/12$	$10/12$

B.10 Domain weights transfer to Qwen2-VL

To explore the generality of **MaD-Mix** across different architectures, we test domain weights obtained from LLaVA-0.5B on Qwen-VL-2B (Wang et al., 2024) in Table 15 with the same setup of Section 4.2. The results show that **MaD-Mix** maintains its benefit compared with other baselines also on Qwen-VL-2B. It would be interesting to further explore the benefit of new domain weights on more model architectures.

C Further comparisons with related works

Data mixing in LMs. Finding a high-quality data composition for LM pretraining is crucial for improved performance. Domain reweighting improves LM downstream performance by rebalancing data contributions from different sources (Brown et al., 2020; Touvron et al., 2023; Blakeney et al., 2024), but manual data mixing is not scalable and may lead to suboptimal domain weights (Albalak et al., 2024; Jiang et al., 2024; Aryabumi et al., 2024). Therefore, some works in the LM field explore the data mixing problems. DoReMi (Xie et al., 2023) employs a small proxy model to redistribute weights across various domains using Group DRO (Sagawa et al., 2019), thereby enhancing the training effectiveness of large base models. Group DRO was also used in (Thudi and Maddison, 2024). DoGE (Fan et al., 2024a,b) employs approximate bilevel optimization to train proxy models for domain weight determination. Recently, (Liu et al., 2024c) employs linear regression models to approximate validation loss across diverse data mixtures by training a large number of very small proxy models. Chen et al. (2024e) create a more general framework with the above methods as specific instantiations. Nevertheless, proxy-based methods necessitate algorithmic modifications in the

Table 15: Transfer domain weights from LLaVA-0.5B to Qwen2-VL-2B for video-image-text instruction tuning.

Benchmark	UNIFORM	AVG	FUSED	MaD-Mix
AI2D	67.78	67.94	67.29	68.26
DocVQA	75.10	75.76	80.11	78.11
InfoVQA	42.69	42.42	42.72	44.02
MathVerse	21.19	18.78	23.73	23.98
MMBench	59.02	56.44	55.33	59.71
MMStar	41.37	42.90	40.89	41.11
MMMU	37.44	36.00	35.98	37.44
ScienceQA	77.89	79.13	77.84	79.23
OCRBench	71.60	73.80	72.90	72.30
RealworldQA	58.82	58.82	58.04	58.69
Video_MMMU	21.02	21.50	20.32	20.83
MVBench	56.38	56.88	56.88	56.92
Average	52.53	52.53	52.67	53.38
Number over UNIFORM	-	7/12	6/12	8/12

training procedure, incurring supplementary proxy computational expenditure when multiple training stages are required, as is the case in VLMs. Moreover, these approaches are limited to small proxy models, which may not be feasible within the context of VLMs with both vision and language models. Other approaches focus on optimizing certain skills, e.g., Chen et al. (2023) introduced a skills-oriented framework for modulation of data mixtures during model training. Thudi et al. (2025) use proxy models in a bilevel optimization framework to optimize the data mixture with downstream data samples. Held et al. (2025) propose mixing by estimating influence on downstream performance from each domain and assuming a linear model for the mixture weights. Another line of works featurize the datasets by deriving a compact domain representation, e.g., through clustering Zhang et al. (2025) or pooling Xie et al. (2025). The domain featureizations are then used to optimize dataset compositions, i.e., deciding weights to assign to the components of a combined dataset, through, e.g., correlation with validation set performance (Zhang et al., 2025) or through leverage scores (Xie et al., 2025). Drawing inspiration from scaling law research (Kaplan et al., 2020; Hoffmann et al., 2022), Data Mixing Laws (Ye et al., 2024) characterize the relationship between mixtures through exponential formulations, with other data mixture scaling laws proposed in (Que et al., 2024; Gu et al., 2024b; Jiang et al., 2024; Kang et al., 2024). Overall, these works have shown that choosing the right data mixture in LMs can boost performance significantly in terms of perplexity and downstream tasks’ accuracy. However, these works are limited to LMs and do not consider the challenges posed by VLMs, which require a more complex data mixture strategy due to, e.g., the multimodal nature of the data, missing modalities, and different training pipelines.

Leverage score mixing. Our unimodal scores measure the contribution of each domain w.r.t. the weight vector w optimally fitted on the entire distribution, formulated through the regression task (1) with uniform target values across domains. Other common related learning tasks include ridge leverage scores (RLS). RLS measures the uniqueness of each data point through a weighted norm of the rows of the eigenvector matrix of the covariance. Specifically, RLS aims to find a vector w being orthogonal to all data points except x_i . It can be formulated as regression for each domain i separately with error variables $e_j = \gamma_j - w^\top x_j$, with $\gamma_j = 1$ if $j = i$, 0 otherwise. Xie et al. (2025) assign higher weights to domains with lower RLS, thus employing inverse RLS as a proxy for dominant directions. In our scores, we formulate (1) that seeks w capturing shared structure across the *entire collection* of domain embeddings. This is achieved by assigning a uniform target value for all domains, i.e., $e_i = 1 - w^\top x_i$. Our scores thus have a different objective, which can be analyzed in the following perspectives. (i) Our resulting score directly quantifies domain relevance, allowing for direct reweighting without inversion. This foundational difference in objective allows for a more natural and direct measure of how much each domain contributes to the shared structure in the embeddings. (ii) Our work aims to capture multi-modal couplings in the data domains. Our new direct formulation (1) facilitates the construction of the multi-modal objective. By introducing shared latent variables α_i via the Fenchel-Young inequality (2), we achieve principled coupling across multiple modalities in the dual formulation, whereas Xie et al. (2025) cannot easily achieve such extension through the inverse RLS.

Data strategies for VLMs. Data mixtures in VLMs are typically hand-picked by the model developers based on intuition or large grid searches, and no systematic approach is used to select the training data mixture. Qwen-VL (Bai et al., 2023a) employs a three-stage training pipeline utilizing a multilingual and multimodal corpus. The pre-training data is task-specific, e.g., captioning and OCR data. In the instruction tuning stage, they combine multi-modal and text-only dialogue to maintain language capabilities performance. LLaVA (Liu et al., 2023a; Li et al., 2024a; Liu et al., 2024a) additionally integrates LLM-generated instruction-following data with visual inputs. They openly release the LLaVA-OneVision (Li et al., 2024a) datasets as collections of domain-specific data, which we use in our experiments. Bunny (He et al., 2024) emphasizes the importance of high-quality data curation. Their approach focuses on finding coresets of the training dataset to improve model performance by removing uninformative image-text pairs. SAIL-VL (Dong et al., 2025) constructs a high-quality dataset through recaptioning via existing frontier VLMs. This curated dataset facilitates effective pretraining and fine-tuning of VLMs across various scales. Previous data selection works on CLIP training include, e.g., CiT (Xu et al., 2023), which proposes a dynamic data curation method coupling a data objective into the learning process by measuring the similarity between text embeddings and task-specific metadata; and, SIEVE (Mahmoud et al., 2024), which introduces a dataset pruning technique using synthetic captions generated by image-captioning models, allowing to identify and remove noisy or misaligned samples, enhancing dataset quality. Data strategies for VLMs have also been studied, e.g., data cleaning, toxicity removal, deduplication; see (Bai et al., 2024) for a comprehensive survey. DataComp (Gadre et al., 2023) deals with data filtering. Infinity-MM (Gu et al., 2024a) investigates the scaling of multimodal models by increasing both model capacity and training data volume. W.r.t. integrating multiple modalities more in general, this is a long-standing challenge in machine learning (Baltrušaitis et al., 2019; Huang et al., 2023; Li et al., 2024d). Simple fusion methods, such as early fusion via concatenation (Barnum et al., 2020) or late fusion by ensembling (Boulahia et al., 2021; Li and Tang, 2024), are often used. Another strategy is to learn a shared latent space where modalities are mapped to, enabling tasks like cross-modal retrieval (Liu et al., 2023a; Zhu et al., 2023), using contrastive learning (Radford et al., 2021; Alayrac et al., 2022) or duality (Houthuys et al., 2018; Tao et al., 2024). Other methods utilize attention to represent interaction between modality-specific encoders (Lu et al., 2019; Cai et al., 2024). Overall, the composition of training data is crucial for the performance of VLMs. To avoid reliance on expensive iterative performance measurements, our work introduces a method that can automatically assign appropriate resampling weights to each multi-modal domain of VLM training data.